Spring 5-1-2015

Aqueous Raft Polymerization of Glycopolymers for Peptide Interaction Studies and Antimicrobial Peptide Mimics for Antimicrobial Activity and Selectivity Studies

Sarah Elizabeth Exley
University of Southern Mississippi

The University of Southern Mississippi

AQUEOUS RAFT POLYMERIZATION OF GLYCOPOLYMERS FOR PEPTIDE INTERACTION STUDIES AND ANTIMICROBIAL PEPTIDE MIMICS FOR ANTIMICROBIAL ACTIVITY AND SELECTIVITY STUDIES

by

Sarah Elizabeth Exley

Abstract of a Dissertation
Submitted to the Graduate School
of The University of Southern Mississippi
in Partial Fulfillment of the Requirements
for the Degree of Doctor of Philosophy

May 2015

ABSTRACT

AQUEOUS RAFT POLYMERIZATION OF GLYCOPOLYMERS FOR PEPTIDE INTERACTION STUDIES AND ANTIMICROBIAL PEPTIDE MIMICS FOR ANTIMICROBIAL ACTIVITY AND SELECTIVITY STUDIES

by Sarah Elizabeth Exley

May 2015

The first section of this work describes the synthesis and characterization of novel glycopolymers synthesized to model GM1 gangliosides, a glycolipid found in neuronal cells. Glucose and galactose were attached to N-hydroxyethyl acrylamide, using chemistry that granted control over the stereochemistry at the C1' carbon of each saccharide, and polymerized via aqueous RAFT (aRAFT). Homopolymers, targeting either 30 or 300 DP, and copolymers, with N-dimethyl acrylamide, were prepared as a glycopolymer platform for investigation of amyloid β (Aβ), a naturally occurring peptide associated with Alzheimer's disease, aggregation. Aβ aggregation kinetics and aggregate size in the presence of glycopolymer were determined.

The second section of this work describes N-(3-guanadinopropyl)methacrylamide (GPMA) synthesis, homopolymerization and copolymerization with N-(3-aminopropyl) methacrylamide (APMA) using aRAFT. Many naturally occurring AMPs have an abundance of lysine and arginine. GPMA, an arginine mimic, was incorporated into our established acrylamide based antimicrobial peptide (AMP) platform with APMA, a lysine mimic, to increase the activity and selectivity of our AMPs over a wider range of bacteria. Antimicrobial activity, against *E. coli*, *S. aureus*, and *P. aeruginosa,* and selectivity, against human red blood cells and cancer cells, was determined for the

GPMA and APMA homopolymers and copolymers. The effect of GPMA counterion on activity and selectivity was also investigated.

The University of Southern Mississippi

AQUEOUS RAFT POLYMERIZATION OF GLYCOPOLYMERS FOR PEPTIDE INTERACTION STUDIES AND ANTIMICROBIAL PEPTIDE MIMICS FOR ANTIMICROBIAL ACTIVITY AND SELECTIVITY STUDIES

by

Sarah Elizabeth Exley

A Dissertation
Submitted to the Graduate School
of The University of Southern Mississippi
in Partial Fulfillment of the Requirements
for the Degree of Doctor of Philosophy

Approved:

Dr. Sarah E. Morgan
Committee Chair

Dr. Charles L. McCormick

Dr. Daniel Savin

Dr. Derek L. Patton

Dr. Vijay Rangachari

Dr. Karen S. Coats
Dean of the Graduate School

May 2015

ACKNOWLEDGMENTS

This work was supported primarily by the U.S. Dept. of Education GAANN Fellowship Program under Award Number P200A090066. The work was partially supported by the National Science Foundation Award Number OISE-1132079.

I would like to thank my advisor Dr. Sarah Morgan for helping me develop as a scientist. I want to specifically thank her for being perceptive and accommodating of my needs as a student. I could not have completed my career at USM without her. I would also like to thank my supporting committee Drs. Vijay Rangachari, Charles McCormick, Daniel Savin, and Derek Patton for their help and guidance. Drs. Veena Choudhary and Veena Koul, of the Institute of Technology at New Delhi, India, allowed me the fantastic experience of working in a foreign lab and communicating my scientific ideas around the world. Thank you to Hannah Brown, Tyler Brown, and Michaelyn Lux for being inspirational undergraduates that challenged me to be a better mentor.

TABLE OF CONTENTS

LIST OF TABLES

Tables

LIST OF ILLUSTRATIONS

Figures

LIST OF SCHEMES

Schemes

POLYMER ABBREVIATIONS

AcGalEAm	2-(2',3',4',6'-Tetra-O-acetyl-β-D-galactosyloxy)ethyl acrylamide
AcGlcEAm	2-(2',3',4',6'-Tetra-O-acetyl-β-D-glucosyloxy)ethyl acrylamide
GlcEAm	2- (β-D-galactosyloxy)ethyl acrylamide
GlcEAm	2- (β-D-glucosyloxy)ethyl acrylamide
$PGal_{300}$	poly[2-(β-D-galactosyloxy)ethyl acrylamide$_{(100)}$], DP:300
$PGlc_{300}$	poly[2-(β-D-glucosyloxy)ethyl acrylamide$_{(100)}$], DP:300
$PGal_{30}$	poly[2-(β-D-galactosyloxy)ethyl acrylamide$_{(100)}$], DP:30
$PGlc_{30}$	poly[2-(β-D-glucosyloxy)ethyl acrylamide$_{(100)}$], DP:30
$PDMAGal_{300}$	poly[2-(β-D-glucosyloxy)ethyl acrylamide$_{(50)}$-*stat*-dimethyl acrylamide$_{(50)}$], DP:300
$PDMAGlc_{300}$	poly[2-(β-D-glucoosyloxy)ethyl acrylamide$_{(50)}$-*stat*-dimethyl acrylamide$_{(50)}$], DP:300
APMA	N-(3-aminopropyl)methacrylamide
GPMA	N-(3-guanidinopropyl)methacrylamide
PAPMA·Cl	poly[N-(3-aminopropyl) methacrylamide$_{(100)}$], chloride counterion
PGT25·TFA	poly[N-(3-aminopropyl) methacrylamide$_{(25)}$-*stat*-N-(3-guanidinopropyl) methacrylamide$_{(75)}$], trifluoroacetate counterion
PGT75·TFA	poly[N-(3-aminopropyl) methacrylamide$_{(75)}$-*stat*-N-(3-guanidinopropyl) methacrylamide$_{(25)}$], trifluoroacetate counterion
PGT100·TFA	poly[N-(3-aminopropyl) methacrylamide$_{(100)}$], trifluoroacetate counterion
PGT25·Cl	poly[N-(3-aminopropyl) methacrylamide$_{(25)}$-*stat*-N-(3-guanidinopropyl) methacrylamide$_{(75)}$], chloride counterion
PGT50·Cl	poly[N-(3-aminopropyl) methacrylamide$_{(50)}$-*stat*-N-(3-guanidinopropyl) methacrylamide$_{(50)}$], chloride counterion
PGT75·Cl	poly[N-(3-aminopropyl) methacrylamide$_{(25)}$-*stat*-N-(3-guanidinopropyl) methacrylamide$_{(75)}$], chloride counterion
PGT100·Cl	poly[N-(3-aminopropyl) methacrylamide$_{(100)}$], chloride counterion

CHAPTER I

INTRODUCTION

This dissertation focuses on the synthesis and testing of polymers that mimic GM1 gangliosides and antimicrobial peptides. In Chapters II and III, the attachment of glucose and galactose to an acrylamide backbone, with specific β stereochemistry at C1', will be described. The homopolymerization and copolymerization, with N, N-dimethylacrylamide, of the synthesized glucose and galactose monomers using aqueous RAFT polymerization will also be discussed. Aggregation of amyloid β peptides in the presence of the reported polymers will be conferred. Chapters IV and V will investigate the synthesis of a methacrylamide monomer with a guanidinium pendant group. This monomer as well as a methacrylamide with a primary amine will be polymerized into homopolymers and statistical copolymers via aqueous RAFT polymerization. These polymers will then be tested for effective bacterial activity and selectivity.

Aqueous RAFT (aRAFT) will be used to synthesize polymers with precise molecular weights and compositions to allow systematic investigations. aRAFT is an ideal technique for the development of saccharide- and amine-containing polymers with specific distributions, as it is compatible with a wide range of monomers, enables control of molecular weight and polydispersity, allows for a wide range of polymer conformations to be synthesized, and does not require extreme protection/deprotection of substituent groups. Additionally, aRAFT can be performed under aqueous conditions and, unlike other controlled polymerization techniques, is unaffected by charged species, maintaining control throughout the reaction.

In both projects, either an acrylamide or methacrylamide is utilized as the polymer backbone. This was done to impart the desirable chemical attributes of acrylamides/methacrylamides onto our synthetic platforms. Specifically, we designed polymers with acrylamide backbones to increase their hydrolytic stability and solubility. The antimicrobial peptide testing was done at physiological pH (pH 7.4); however, the Aβ investigation was done at pH 8, and the increased stability and solubility of the acrylamide backbone eliminates hydrolysis and precipitation concerns, respectively. Additionally, both projects are designed as platforms for future research, therefore, having an acrylamide/methacrylamide backbone will allow for a more diverse implementation of the developed systems.

CHAPTER II

GLYCOPOLYMER ARCHITECTURES

Chapter Overview

This chapter aims to inform the reader of pertinent literature pertaining to the aggregation of amyloid β (Aβ) peptides in response to the saccharides of GM1 gangliosides, providing the argument and need for the research presented in Chapter III. Briefly, Aβ peptides are implicated in the pathology of Alzheimer's disease, as they are present in the extracellular space of neuronal cells as soluble oligomers or insoluble fibrils that lead to plaque formation. Through interaction with various modulators, Aβ peptides are shown to undergo conformational change and aggregate into toxic species. GM1 gangliosides are reported as modulators that increase and alter Aβ aggregation. The head group of GM1 gangliosides are comprised of several saccharide residues, including glucose and galactose. Efforts have been made to identify the specific influence of glucose and galactose on Aβ aggregation; however, it is difficult to separate the effects of the individual saccharides using traditional biochemical techniques. Circumventive methods, used to evaluate saccharide contribution, resulted in conflicting reports. Finally, polymer research has not demonstrated soluble biorelevant glycopolymers that are stable over a wide range of testing conditions nor used them to evaluate saccharide impact on Aβ aggregation.

Important Literature

Alzheimer's disease (AD) is a neurodegenerative disease that is responsible for approximately 70% of all dementia cases.[1] Elucidation of the pathology of AD is important as it will provide the opportunity for treatment development. AD is

characterized by the progressive degeneration of cognitive and ambulatory abilities and the development of intricate neuropathological features,[2] namely significant loss of neurons and the appearance of senile plaques and neurofibrillary tangles (NFTs).[3] The senile plaques are formed from amyloid fibrils, which are a result of the aggregation of the peptide amyloid-β (Aβ). Aβ is expressed in the extracellular space of the brain and originate from cleavage of the amyloid precursor protein (APP). The most prevalent peptides are Aβ40 and Aβ42, having 40 and 42 amino acid residues, respectively (*Figure 1*).[4] Aβ42 is thought to be the more toxic of the species, and is thus the focus of the present study.[3-4] Aβ aggregates via self-association in a nucleation-dependent manner to form larger molecular weight oligomers and fibrils.

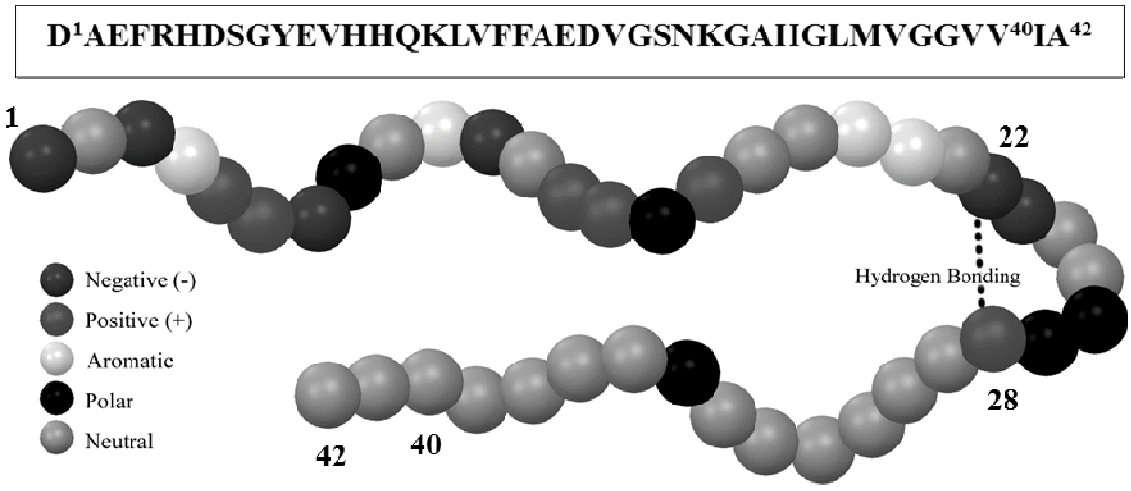

Figure 1. Illustrations detailing the amino acid residues and their corresponding polarity or charge of Aβ monomer. Hydrogen bonding occurs at residues 22, glutamic acid, and 28, lysine, stabilizing the monomer in a β sheet conformation.

Various studies have determined that the soluble oligomeric species of Aβ peptides are the result of an aggregation pathway discrete from that of fibrillogenesis or amyloidogenesis. Gellerman *et al.* determined that not only are the pathways discrete, but interchange between the two aggregate species does not occur, indicating that each

are stable entities.[2] Previous studies in our laboratories demonstrated a similar phenomenon, indicating that two different aggregation pathways exist.[5] Each aggregate species promotes further conformational change and aggregation of monomeric Aβ42 (i.e. like promotes like).[2]

The toxicity of Aβ fibrils are widely debated as there seems to be a disproportionate association between the appearance of fibril plaques and the extent of neurological damage. That is, the brains of people suffering from AD impairment have varying concentrations of fibril plaques, and the plaque level does not directly correlate with the degree of impairment.[5] Additionally, Williams *et al*. determined that the greater the degree of association of the peptide, meaning the more fibril-like it became, the less effective it was as a membrane disruptor, with membrane disruption being one potential cause of neuronal cell death.[2] This lack of correlation suggests that the oligomeric species play a significant role in AD pathology.

Various modulators have been demonstrated to promote conformational changes and aggregation of Aβ peptides. Gangliosides are glycosphingolipids that are composed of a hydrophobic ceramide, consisting of a sphingosine and a fatty acid moiety, hydrophilic sugars and sialic acid moieties (*Figure 2*).[3] Gangliosides are found throughout the brain in varying concentrations. The fraction of GM1 gangliosides has been reported to comprise 0.5-13% w/w of the membrane. With increasing age, the GM1 fraction increases to 15-30% w/w of the membrane. Additionally, cholesterol concentrations in the cell membrane increase with age and promote aggregation and lipid raft formation of GM1 gangliosides. Increase in ganglioside concentration, both locally through lipid rafts and globally through increased ganglioside number, is thought to

promote the shift of common non-toxic monomeric Aβ species to toxic aggregate species.[6] Yanagisawa *et al.* discovered that GM1-bound Aβ peptides are present during early stages of AD pathogenesis and it is hypothesized that the peptides act as "seeds" to polymerize Aβ into mature fibrils and senile plaques.[7] Choo-Smith *et al.* observed that Aβ40 interacted with micellar GM1-gangliosides and as a result of the interaction, Aβ40 underwent a conformational change characterized by a conformational change from randomly coiled to cross β-sheet structure.[8] The hydrophobic, apolar C-terminal region of Aβ40 was suggested to be paramount for interaction with GM1-gangliosides. The authors hypothesized that Aβ interaction with gangliosides could induce membrane perturbation that ultimately leads to neuronal cell death.[8-9] Recently, however, Yamamoto *et al.* determined that different variants of Aβ peptides bind to different types of gangliosides;[10] though, the reason has yet to be fully understood. The primary differences between the various types of gangliosides are the types and distributions of saccharides present in the hydrophilic head group and the number of sialic acid moieties present. Sialic acids have been extensively studied and their affects are known.[11] Therefore, the preferential binding of the variant Aβ peptides to specific gangliosides must result from the different types and distributions of saccharides present within each respective ganglioside.

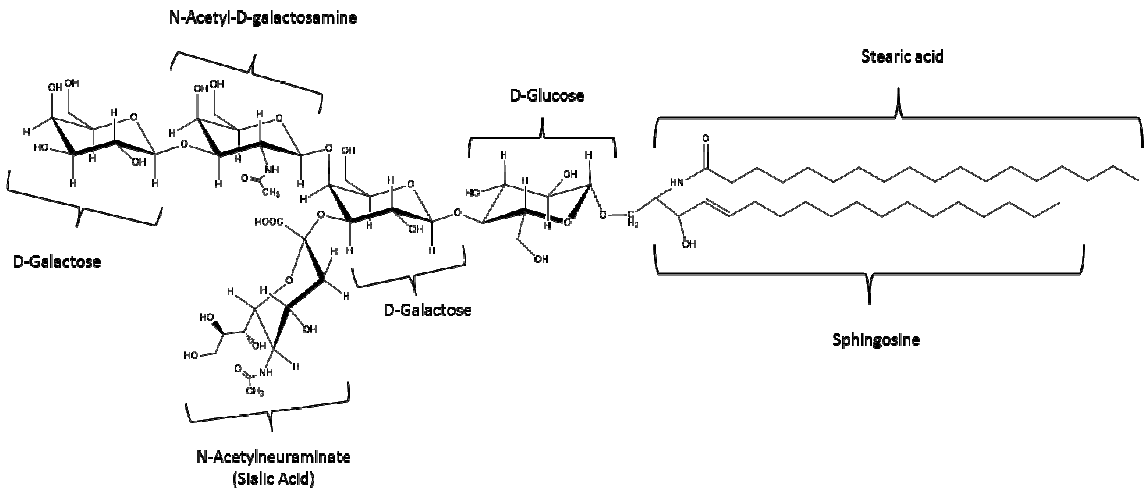

Figure 2. An illustration of GM1 ganglioside, with all components appropriately labelled.

To date, little has been accomplished to elucidate the influence of individual saccharides on the aggregation mechanisms of Aβ42. Fung *et al.* studied the effect of simple carbohydrates on the aggregation and fibrillogenesis of Aβ42 by observing secondary and quaternary conformational changes in relation to the presence of individual saccharides.[12] They concluded that the secondary structure was affected by glucose and sucrose and that the hydrogen bonding pattern unique to each saccharide is crucial in the development of Aβ42 structure. Matsumoto *et al.* analyzed saccharide-Aβ42 binding affinities as well as saccharide-induced peptide conformational change and aggregation through the development of self-assembled monolayers (SAMs) of saccharides, which were entitled sugar microarrays.[13] The various saccharides, including N-acetyl-β-D-glucosamine (β-GlcNAc), β-galactose (β-Gal), α-mannose (α-Man), β-glucose (β-Glc), 6-sulfo-β-D-glucosamine (6-sulfo-β-D-GlcNAc) and sialic acid were attached to a substrate through click chemistry. It was determined that Aβ42 had the strongest binding affinity towards 6-sulfo-β-D-GlcNAc followed by sialic acid, β-Gal, β-Glc, β-GlcNAc, and α-Man.

Synthesis of soluble glycomonomers and glycopolymers has been documented in the literature, though not for Aβ aggregation research. We previously reported the attachment of D-glucuronic acid sodium salt to aminopropyl methacrylamide for polymerization via aRAFT.[14] The addition was successful; however, this, like many other glyco-systems,[15] utilized chemistries that remove a portion of the biological relevance, as the attachment of D-glucuronic acid sodium salt resulted in glycomonomer pendant to the polymer backbone through a nitrogen rather than an oxygen, and stereochemical control at C1' was not obtained. McCormick *et al.* reported kinetic data for the homopolymerization and chain extension of a methacrylate glycan monomer via aRAFT, using a dithioester chain transfer agent (CTA).[15b] Ambrosi *et al.* reported the synthesis and the free radical polymerization of glucose and galactose functionalized methacrylates with retention of β stereochemistry at C1'.[16] Parry *et al.* synthesized a methacrylamide glycan monomer that maintained α stereochemistry at C1' and was polymerized via RAFT in a DMF:H_2O mixture using a dithioester as the chain transfer agent.[17]

To our knowledge, the synthesis of acrylamide based glycomonomers with controlled stereochemistry at the C1' carbon and their polymerization via aRAFT have not been previously reported. Additionally, the effects of glucose and galactose on the aggregation of Aβ have not been clearly established. Previous studies, using simple sugars and sugar microarrays, show contradictory results,[12-13] and appropriate biorelevant concerns are not considered, such as (1) stereochemistry of the sugar to monomer attachment, and (2) concentration and localization of the representative saccharides. Finally, investigation of the aggregation processes of Aβ species formed in the presence

of soluble glycopolymers has not yet been reported. In this paper, synthesis of galactose and glucose glycomonomers with an acrylamide backbone, is detailed, as well as the RAFT controlled homo- and co-polymerization of N-dimethyacrylamide, 2- (β-D-galactosyloxy)ethyl acrylamide (GalEAm) and β-glucosyloxy)ethyl acrylamide (GlcEAm). Aβ aggregation testing in the presence of glycopolymers, done through ThT fluorescence and SDS-PAGE is also described.

CHAPTER III

EXPERIMETAL DETAIL FOR GLYCOPOLYMER ARCHITECTURES

Research Overview

From previously reported results, it is clear that gangliosides present in the lipid bilayer of eukaryotic cells, when in sufficient concentrations, provoke aggregation of Aβ peptides. Sialic acids as well as a ceramide tail are present in all gangliosides, leaving differences in saccharide moieties and distribution as the only differentiable characteristics between gangliosides. Unfortunately, control over sugar chemistry in biomacromolecules is very difficult, with the isolation of a specific saccharide and saccharide distribution being nearly impossible utilizing traditional biochemical techniques. To alleviate these difficulties, this project aimed to generate synthetic polymer models with glucose and galactose, as pendant groups, through the use of aRAFT controlled radical polymerization to develop a fundamental understanding of how Aβ peptides interact with saccharides on GM1 gangliosides. aRAFT polymerization will be employed to achieve the specificity needed to properly evaluate the effects of saccharides. The results from these studies will help to resolve the previously reported contradictory findings for Aβ peptide-saccharide aggregation. In this chapter the synthesis of galactose and glucose glycomonomers with an acrylamide backbone, is detailed, as well as the RAFT controlled homo- and copolymerization of N-dimethyl acrylamide, 2- (β-D-galactosyloxy)ethyl acrylamide (GalEAm) and β-glucosyloxy)ethyl acrylamide (GlcEAm). Aβ aggregation testing in the presence of glycopolymers, done through ThT fluorescence, and SDS-PAGE and immunoblotting, is also described.

Objectives of Research and Research Questions

This project aimed to develop a synthetic polymer platform that mimics the saccharide head groups of gangliosides for investigation into Aβ peptide aggregation and future saccharide related environmental questions. The goal of this project was achieved through several research objectives and questions:

I. Glycomonomers synthesized with correct stereochemistry at the C1' carbon of either glucose or galactose.
   a. *Can sufficient yield be obtained for the addition of HEAm to dehalogenated saccharide despite the inherent tendency for HEAm to retain water, which when present generates a competitive reaction?*

II. Glycomonomers polymerized into homo- and statistical copolymers, with N, N-dimethyl acrylamide via aqueous RAFT.
   a. *Does the steric properties of the bulky saccharide affect the ability of RAFT to control the molecular weight and PDI when higher MW glycopolymers are targeted?*
   b. *Will copolymerization of the glycomonomers with DMA result in a statistical distribution of each monomer?*

III. Aβ peptides aggregation monitored in response to each (glyco)polymer and compared to Aβ peptides aggregation in environments free of (glyco)polymers and other aggregation affecting agents.
   a. *Do our considerations for biorelevance result in a clear answer for the environmental effect of saccharides on Aβ peptides, resolving conflict in previous research?*

b. *Does the stereochemistry of the C4' carbon, which separates glucose and galactose, provide enough of a change in environment to alter the aggregation of Aβ peptides?*

Materials and Methods

Materials

For protected glycomonomer synthesis, acetobromo-α-galactose, ≥95% (AcGal) (Sigma-Aldrich, USA), acetobromo-α-glucose, ≥95% (AcGlc) (Sigma-Aldrich, USA), silver trifluoromethanesulfonate, >99% (silver triflate) (Sigma-Aldrich, USA), sodium sulfate, >99% anhydrous (Sigma-Aldrich, USA), and powdered 3Å molecular sieves (Sigma-Aldrich, USA) were used as purchased. *N*-Hydroxyethyl acrylamide (HEAm) (Sigma-Aldrich, USA) was filtered through neutral aluminum oxide (Sigma-Aldrich, USA) to remove the inhibitor. Dichloromethane (DCM) (Sigma-Aldrich, USA) was distilled from calcium carbonate under nitrogen gas. For glycomonomer deprotection, sodium methoxide, 30 wt% in methanol (Sigma-Aldrich, USA), methanol, 98.8% anhydrous (MeOH) (Sigma-Aldrich, USA), and Dowex® 50WX2 (Sigma-Aldrich, USA) were used as purchased. Polymerization utilized sodium acetate, >99% anhydrous (Sigma-Aldrich, USA), and acetic acid, glacial (Fisher Scientific) for a 0.11M buffer (0.025 M acetic acid, 0.075 M sodium acetate). *N,N*-Dimethylacrylamide (DMA) (Sigma-Aldrich, USA) was distilled, under vacuum, to remove the inhibitor. Additionally, 4,4'-Azobis(4-cyanovaleric acid), ≥98% (V-501) (Sigma-Aldrich, USA) was used as the initiator. 4-cyano-4-(ethylsulfanylthiocarbonylsulfanyl)pentanoic acid (CEP) was used as the chain transfer agent (CTA) and was synthesized via previously published procedures.[18] For testing with Aβ peptides, Aβ 42 was synthesized by and

purchased from the Peptide Synthesis Facility at the Mayo Clinic (Rochester, MN) using routine Fmoc (*N*-(9-fluorenyl) methoxycarbonyl) chemistry. MALDI-TOF mass spectrometry revealed >90% purity of the peptide. Sodium dodecylsulfate (SDS) and thioflavin-T (ThT) were procured from Sigma-Aldrich (USA). All other chemicals were obtained from VWR Inc.

Synthesis of 2-(2',3',4',6'-Tetra-O-acetyl-β-D-galactosyloxy)ethyl acrylamide (AcGalEAm) and 2-(2',3',4',6'-Tetra-O-acetyl-β-D-glucosyloxy)ethyl acrylamide (AcGlcEAm).

Elimination of water was paramount for the successful synthesis of AcGalEAm and AcGlcEAm; therefore, all glassware was heated in an oven at 140°C for 30 minutes and cooled under nitrogen. AcGal or AcGlc (26 g, 65 mmol) was added to a solution of HEAm (5 eq.) and 5% powdered molecular sieves in DCM (1000 mL), while stirring under nitrogen for one hour. Silver triflate (1.5 eq.) was then added, maintaining a positive pressure of nitrogen, and then the mixture was allowed to stir for 24 hours (*Scheme 1*). After addition of silver triflate, the positive pressure of nitrogen was removed and the reaction mixture was kept under closed conditions, maintaining an air free environment. The appearance of a gray/purple sediment indicated the progress of the reaction, as silver bromide, a light sensitive byproduct, precipitated. The final solution was filtered, washed with 1M HCl (3x), to remove excess HEAm, and dried over sodium sulfate. Rotary evaporation and lyophilization resulted in a faintly peach colored solid (Yield: ~70%). AcGalEAm, ^{1}H NMR (300 MHz, DMSO): δ [ppm] 2.00, 2.06, 2.16 (d, m, m; 12H-m, n, o, p); 3.52 (m; 2H-e); 3.60, 3.75 (m, m; 1H-d, 1H-d); 3.92 (m; 1H-l); 4.14 (m; 1H-k); 4.48 (m; 1H-k); 5.02 (d of d; 1H-j); 5.20 (m, 1H-g); 5.40 (t; 1H-h); 5.67

(d of d; 1H-a); 6.10 (m; 1H-b); 6.31 (m; 1H-C). AcGlcEAm, ^{1}H NMR (300 MHz, DMSO): δ [ppm] 2.06 (m, 12H-m, n, o, p); 3.56 (m, 2H-e); 3.73, 3.89 (m, m; 1H-d, 1H-d); 4.14 (m, 1H-l); 4.24 (m; 1H-k); 4.52 (m; 1H-f); 4.99 (m; 1H-j); 5.10 (m, 1H-g); 5.22 (m; 1H-h); 5.66 (d of d; 1H-a); 6.13 (m; 1H-b); 6.30 (m, 1H-c).

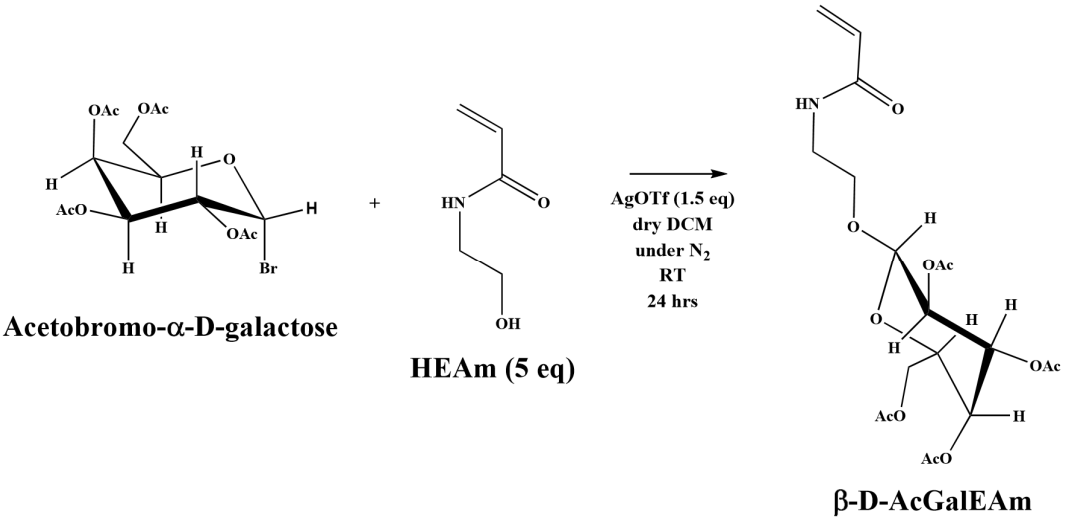

Scheme 1. Synthesis of AcGalEAm. The same conditions were employed to prepare AcGlcEAm.

2- (β-D-galactosyloxy)ethyl acrylamide (GalEAm) 2- (β-D-glucosyloxy)ethyl acrylamide (GlcEAm).

AcGalEAm and AcGlcEAm were deacetylated by an established procedure.[16] Sodium methoxide (1 mL per 10 mL of solvent) was added to a solution of either AcGAlEAm or AcGlcEAm in methanol, while it stirred under nitrogen, and the mixture was allowed to react for 40 minutes (*Scheme 2*). Dowex® 50WX2 was then added to the reaction mixture to absorb sodium cations and neutralize the solution and allowed to stir for 15 minutes. A faintly peach colored, hygroscopic solid was obtained after filtration, rotary evaporation and lyophilization. GalEAm, ^{1}H NMR (300 MHz, D_2O): δ [ppm] 3.2-

3.8 (m; 10H-d', e', f', g', h', i', h', k', l'); 4.20 (d, 1H-f'); 5.56 (d of d; 1H-a'); 6.03 (m; 1H-c', 1H-b'). GlcEAm, ^{1}H NMR (300 MHz, D_2O): δ [ppm] 3.0-3.85 (m; 10H-d', e', f', g', h', i', h', k', l'); 4.27, 5.02 (d of d, d of d; (1H-f'); 5.57 (d of d; 1H-a'); 6.04 (m; 1H-c', 1H-d').

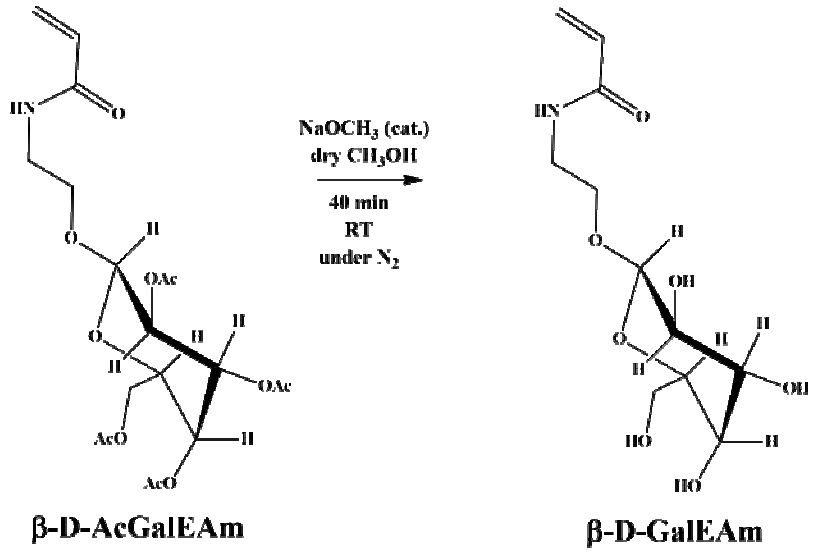

Scheme 2. Deacetylation of AcGalEAm to form the desired monomer, GalEAm. The same conditions were utilized to form GlcEAm.

Aqueous RAFT Polymerization of Glycopolymers.

Utilizing aqueous RAFT polymerization, polymer molecular weights were targeted by selecting appropriate initial monomer and CTA concentrations. The ratio of M_0:CTA_0 was set to be approximately 500:1 and 100:1, with an expected conversion of 60% and 30%, to yield a degree of polymerization of ~300 and 30, respectively. The monomer concentration of the reaction was 0.5 M. V-501 was used as the initiator. For polymerizations targeting a DP of 300, CEP was used as the chain transfer agent (CTA) at a ratio of CTA_0:I_0 of 5. For polymerizations targeting a DP of 30, CEP was used at a ratio of CTA_0:I_0 of 10. The polymerization took place in 0.1 M sodium acetate buffer

(pH 5), with benzene sulfonic acid as an internal standard (25 mg), at 70°C.[19] Methanol was added in low quantities (200 μL) to improve the solubility of CEP in the aqueous media (*Scheme 3*). After the completion of the reaction, the solutions were quenched in liquid nitrogen and exposed to air. Each solution was then dialyzed against water for 72 hours, lyophilized for 72 hours and then stored in desiccant until testing. For the purpose of this paper, polymers are referred to as either PGal or PGlc to identify homopolymers of GalEAm or GlcEAm, respectively. The subscript number, as in $PGal_{300}$, indicates the targeted degree of polymerization.

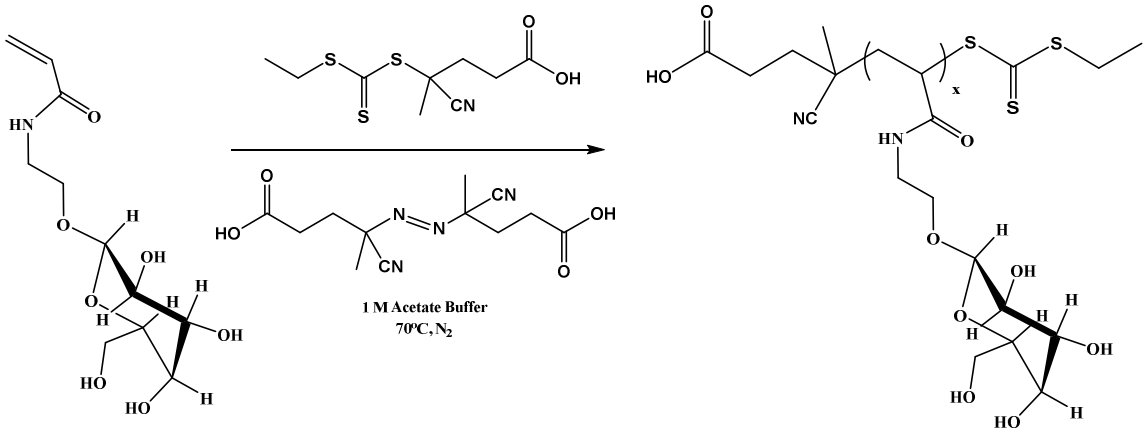

Scheme 3. Representative aqueous RAFT polymerization of GalEAm. Identical conditions were used for all homo- and copolymerizations. The CTA, on top of the reaction arrow, is CEP and the initiator, below the reaction arrow, is V-501.

Nuclear Magnetic Resonance (NMR)

^{1}H NMR was performed with a Varian Mercury^{PLUS} 300 MHz spectrometer in $CDCl_3$, utilizing delay times of 2 s to confirm monomer synthesis and identify the structures of PGal, and PGlc homopolymers, and the PDMA-*stat*-PGal/PDMA-*stat*PGlc copolymers. 64 scans were taken for each experiment with a 3.1 second recycle delay. For each of the homopolymers, unique peak assignments were made, and the copolymer compositions were calculated for the statistical polymer via peak integration. ^{1}HNMR

was also performed on aliquots taken at intervals from reaction mixtures to monitor conversion and ensure linearity of monomer conversion with time. Conversion was determined through comparative integration of the internal standard, benzene sulfonic acid, and the vinylic peaks.

Mass Spectrometry

In order to determine the molecular weight of synthesized AcGalEAm (m/z: 445 + 23 (Na)), AcGlcEAm (m/z: 445 + 23 (Na)), GalEAm (m/z: 277 + 23 (Na)) and GlcEAm (m/z: 277 + 23 (Na)), mass spectroscopy was done on a ThermoFinnigan (San Jose, CA) TSQ 7000 triple-quadrapole instrument that was equipped with an electrospray ionization source (ESI). The capillary temperature was maintained at a temperature of 200°C, with a voltage of 20 V. The electrospray needle voltage was 4.7 kV, and the tube lens was maintained between 70 and 100 V. Samples were injected into the ESI source as a methanol/water (1:1) solution that had sodium chloride to charge the polymers. The solutions were injected at a rate of 10 μL/sec. All data was analyzed using Xcalibur (Fischer-Scientific, Inc.) software.

Matrix-Assisted Laser Desorption Ionization (MALDI) Time of Flight Spectrometry

MALDI-ToF was used to determine the molecular weight and polydispersity of all synthesized glycopolymers. All MALDI was done on a Bruker Microflex, equipped with a 337 nm nitrogen laser in linear mode and 20 kV accelerating voltage. The detector gain was set at 5.0x. Pulsed ion extraction (800 ns and 360 ns for higher and lower MW polymers, respectively) was used during the collection of all data. An average of 100 laser shots was obtained for each polymer. Two poly(styrene) standards, 4,000 g/mol and 50,000 g/mol, were used as external calibration standards. Plates were spotted using a

thin layer by layer deposition technique. 2,5-Dihydroxybenzoic acid (Sigma-Aldrich, USA), used as the matrix, was dissolve in HPLC grade THF (50 mg/mL) and then spotted onto the MALDI plate. Prompt evaporation of THF, via blowing, was used to obtain small crystals. Each glycopolymer was then dissolved in HPLC grade water (1 mg/mL) and spotted on top of the dried DHB matrices. A heat gun was used to promote rapid evaporation of water and create smaller glycopolymer crystals.

Amyloid-β Peptide Isolation

Lyophilized stocks of synthetic Aβ 42 were stored at -20 °C desiccated. Briefly, 1.5–2 mg of peptide was dissolved in 0.5 ml of 30 mM NaOH and stored for 15 min at room temperature prior to size exclusion chromatography (SEC) onto a 1X30-cm Superdex-75 HR 10/30 column (GE Healthcare) attached to an ÄKTA FPLC system (GE Healthcare) to remove any preformed aggregates, as reported previously.[20] The column was pre-equilibrated in 20 mM Tris-HCl (pH 8.0) at 25 °C and run at a flow rate of 0.5 ml/min. One-minute fractions were collected. Concentrations of Aβ were determined by UV-visible spectrometry on a Cary 50 spectrophotometer (Varian Inc.) using a molar extinction coefficient of 1450 cm^{-1} M^{-1} at 276 nm (ExPASy) corresponding to the single tyrosine residue in Aβ 42. Peptide integrity after SEC was again confirmed by MALDI-ToF mass spectrometry, which showed a monoisotopic molecular mass of 4516.31 Da, in good agreement with a calculated mass of 4513.13 Da. Monomeric Aβ 42 fractions were stored at 4°C and used within 2–5 days of SEC purification in all experiments to avoid any preformed aggregates in our reactions.

Thioflavin Fluorescence Spectroscopy (ThT Fluorescence)

ThT fluorescence assays were performed as previously reported.[5] Briefly, 5 μL aliquots of reactions were diluted with 70 mL of 10 μM ThT in 20 mM Tris, pH 8.0 in a quartz microcuvette. ThT fluorescence was performed by exciting at 450 nm and monitoring the emission at 482 nm in kinetic mode for 1 min with excitation and emission slits were set at 10 nm.

Polyacrylamide Gel Electrophoresis (PAGE)

Samples were dissolved in loading buffer (1X Laemmli buffer) containing 1% sodium dodecyl sulfate (SDS), applied without heating to 4–20% Mini-PROTEAN TGX gels (Biorad) containing bis-Tris, and resolved in Laemmli running buffer with 0.1% SDS. Dye-linked molecular mass markers (Blue Plus2 Prestained Standards, Invitrogen) were run in parallel for calibration. Gels were visualized using a silver stain kit (Pierce) following standard protocols provided from the manufacture.

Results and Discussion

Monomer and Polymer Synthesis

AcGlcEAm and AcGalEAm glycomonomers were synthesized using a modification of the procedure reported by Ambrosi *et al.*[16] as described in the experimental section and illustrated in *Scheme 1*. We chose to synthesize acrylamide-based glycomonomers, rather than the methacrylate monomers studied by Ambrosi *et al.*, to take advantage of their ready polymerization in aqueous solution under moderate reaction conditions, hydrolytic stability, solubility over a range of pH and salt concentrations, and relatively simpler purification. In our system, silver triflate was substituted for silver carbonate in the traditional Koenigs-Knorr reaction. The reactions

were performed at room temperature over a period of 24 hours and excess HEAm was removed through acid washes, leaving the saccharide functionalized acrylamide, AcGalEAm and AcGlcEAm, in the organic layer (^{1}H NMR in *Figures 3* and *4,* yield 70%). In the Ambrosi methacrylate system, on the other hand, -40°C reaction conditions, increased reaction time of 48 hrs, and product purification by column chromatography were required. They polymerized protected and deprotected monomer and concluded that deprotection of the monomer prior to polymerization resulted in better removal of the acetyl groups. Due to the increased hydrolytic stability of the amide linkage in our acrylamide system, concern over the decomposition of the monomer during deprotection was eliminated. Sodium methoxide in methanol was used to remove the acetyl protecting groups, and complete deacetylation occurred without loss of product (*Figures 5* and *6*). To our knowledge, this is the first report of the synthesis of an acrylamide glycomonomer with a specific attachment at the C1' carbon of either glucose or galactose.

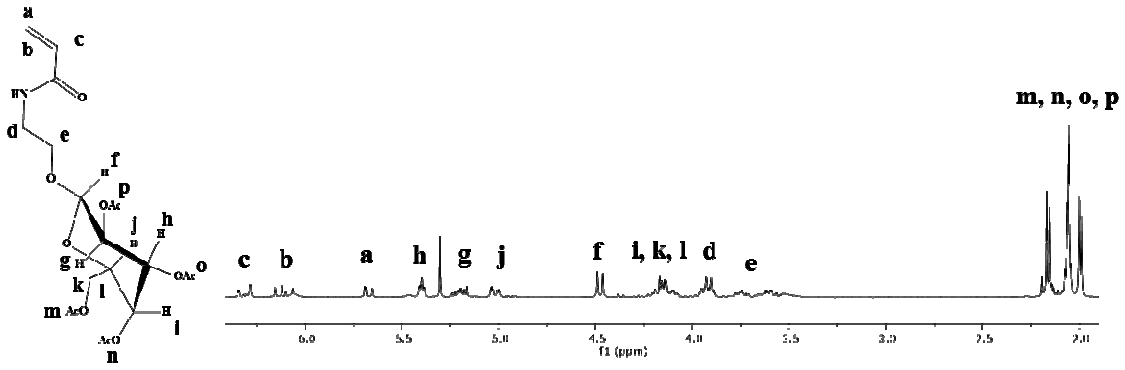

Figure 3. ^{1}H NMR, in deuterated chloroform, of AcGalEAm, with proton peaks assigned.

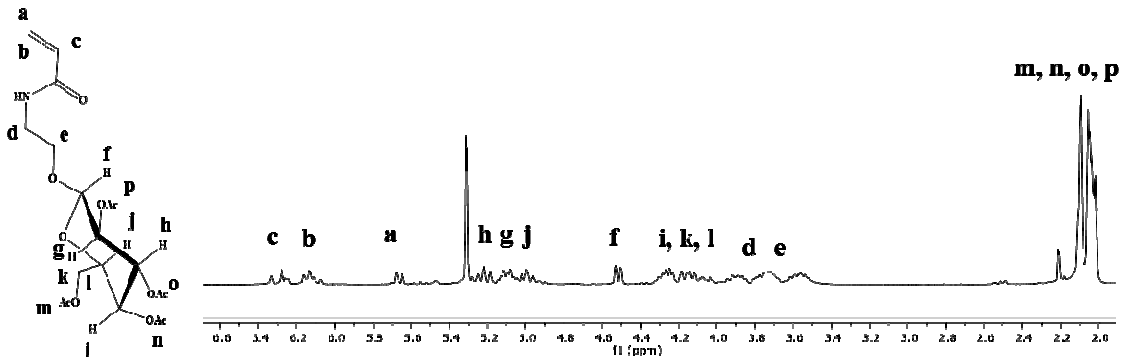

Figure 4. [1]H NMR, in deuterated chloroform, of AcGlcEAm, with proton peaks assigned.

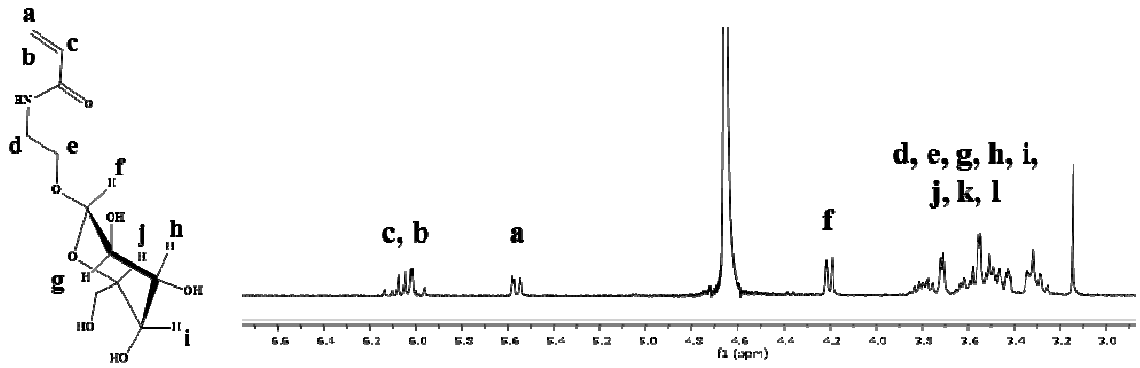

Figure 5. [1]H NMR, in deuterated water, of GalEAm after de-protection with proton peaks assigned.

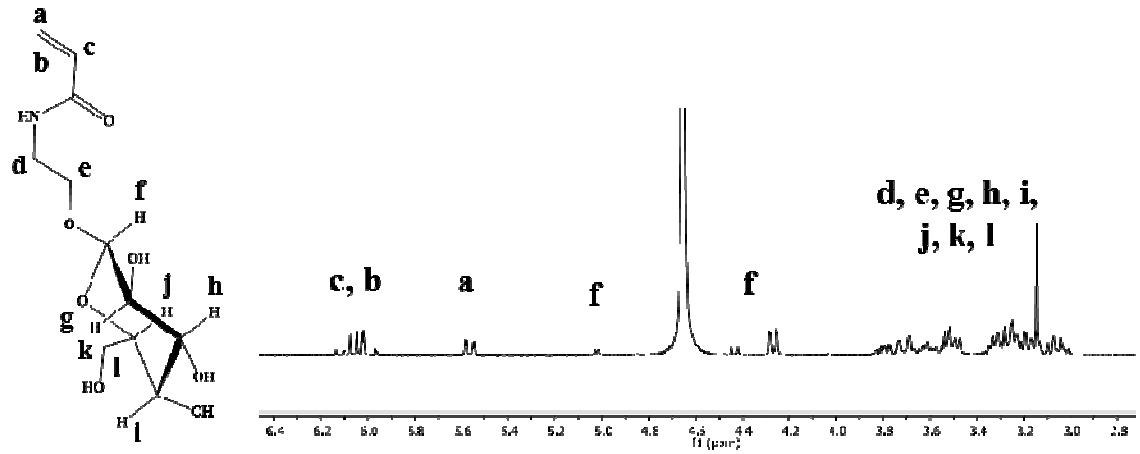

Figure 6. [1]H NMR, in deuterated water, of GlcEAm after de-protection with proton peaks assigned.

Confirmation of the stereochemistry at the C1' carbon was achieved through ^{1}H NMR analysis. Bubb *et al.* identified the proton peaks correlating to the α and β enantiomers for glucose modified at the C1' carbon.[21] With this knowledge and a ^{1}HNMR of enantiomeric D-glucose and D-galactose, identification of the proton peaks correlating with the α- and β-enantiomers of synthesized monomers was easily determined. *Figure 7* shows ^{1}HNMR spectra of D-galactose (upper) and GalEAm (lower), where the peak for the α-enantiomer for galactose appears around 5.0 ppm and the β-enantiomer proton peak is located around 4.20 ppm. *Figure 8* shows a similar comparative spectrum for D-glucose and GlcEAm. Integration of the α and β proton peaks for GalEAm (*Figure 7*) and GlcEAm (*Figure 8*), showed that 98% and 88%, respectively, of the monomers had the desired β orientation at C1'. It is possible that the GlcEAm showed less stereochemical control than the GalEAm because of neighboring group effects in glucose, which has the C4' hydroxyl group equatorially positioned and may sterically affect the β-enantiomer.

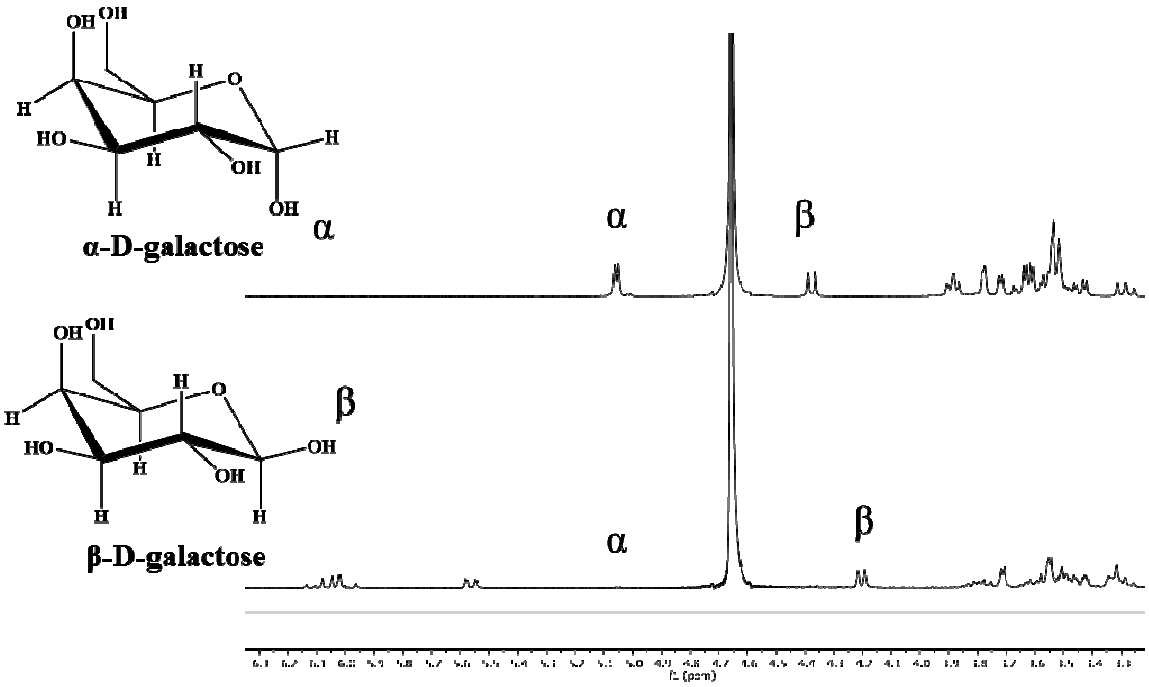

Figure 7. Representative ^{1}H NMR showing C1' stereochemistry of stock D-galactose (upper) as compared to synthesized GalEAm (lower), where GalEAm has 98% of the desired β-linkage.

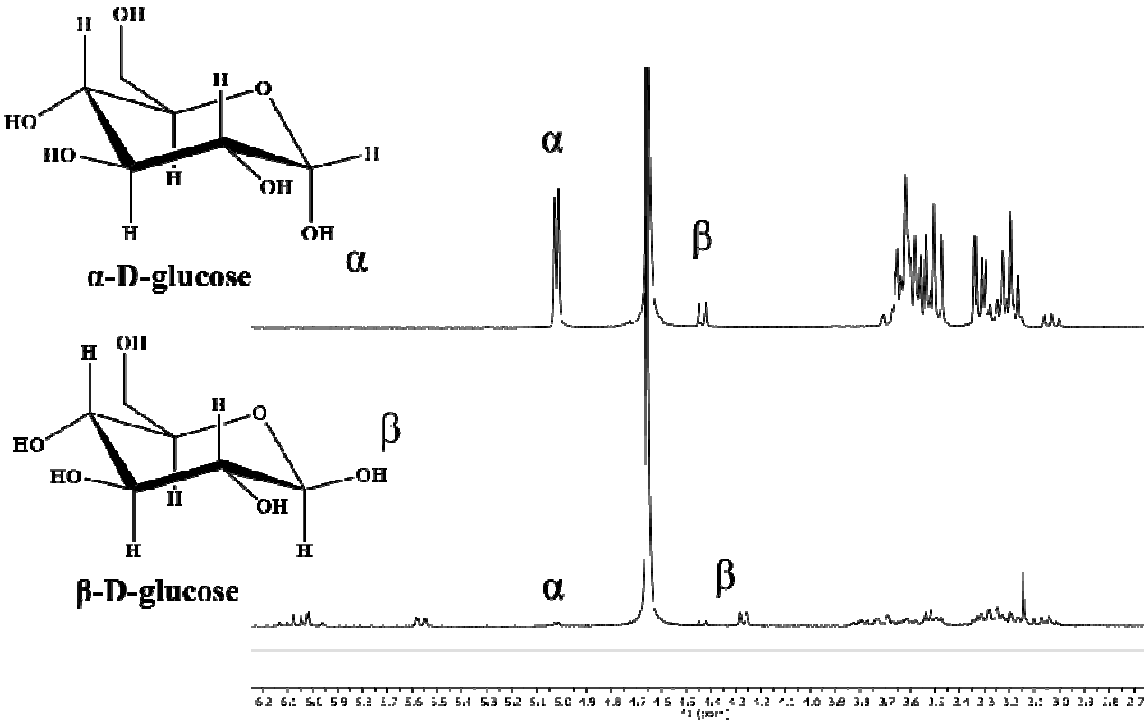

Figure 8. Representative ^{1}H NMR showing C1' stereochemistry of stock D-glucose (upper) as compared to synthesized GlcEAm (lower), where GlcEAm has 88% of the desired β-linkage.

Four homopolymers of GalEAm and GlcEAm at differing molecular weights and copolymers of DMA with GalEAm and GlcEAm were synthesized via aRAFT polymerization, following the reaction procedure outlined in *Scheme 3*. In *Table 1* is a summary of the theoretical MWs. *Figures 9, 10, 11 and 12* are representative ^{1}H NMR spectra of $PGal_{300}$, $PGlc_{300}$, $PDMAGal_{300}$ and $PDMAGlc_{300,}$ respectively. The vinyl peaks of the monomers are no longer present and are replaced by methylene peaks of the polymer backbones at 1.0 - 2.0 ppm, indicating successful polymerizations. Furthermore, unique peaks of d', e' (2.8 ppm) for DMA and d, e, g, h, i, j, k, l (3.0-3.9 ppm) for both GalEAm and GlcEAm (*Figures 11* and 12, respectively) were identified and integrated to determine the mol% of monomers in each copolymer. As indicated in *Table 1*,

incorporation for all monomers was close to the theoretical prediction, with GalEAm and GlcEAm representing 37% and 32% of their respective copolymers.

Table 1

Summary of aRAFT polymerized glycopolymers

Polymer	Mn_{th}(g/mol)[a]	mol% $Sugar_{exp}$
1. $PGal_{300}$	88,000	100
2. $PGal_{30}$	8,500	100
3. $PGlc_{300}$	79,000	100
4. $PGlc_{30}$	7,500	100
5. $PDMAGal_{300}$	50,700	37[b]
6. $PDMAGlc_{300}$	110,200	3

[a]Theoretical calculations based upon $[M_o]/[CTA]$. [b]Theoretically, 56 mol% DMA and 44 mol% GalEAm. [c]Theoretically, 61 mol% DMA and 39 mol% GlcEAm.

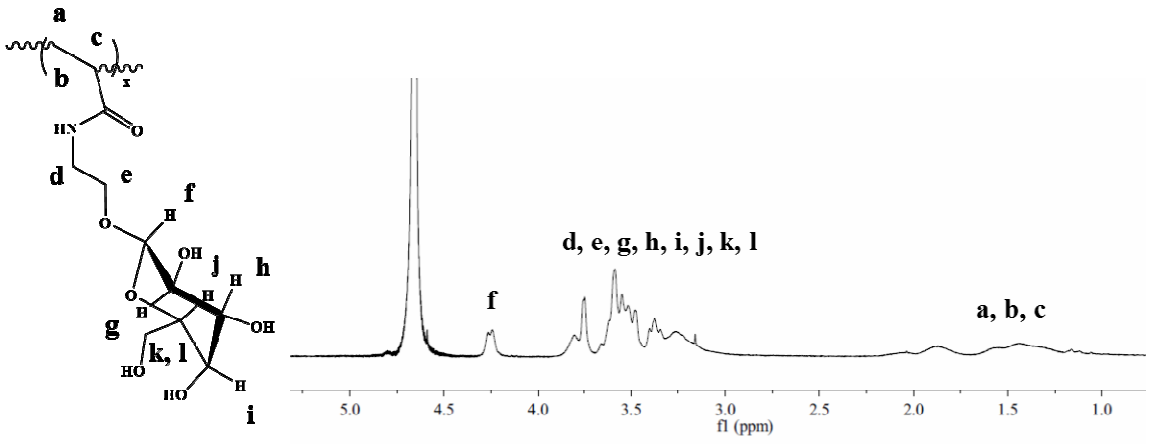

Figure 9. Representative ^1H NMR, in deuterated water, of $PGal_{300}$.

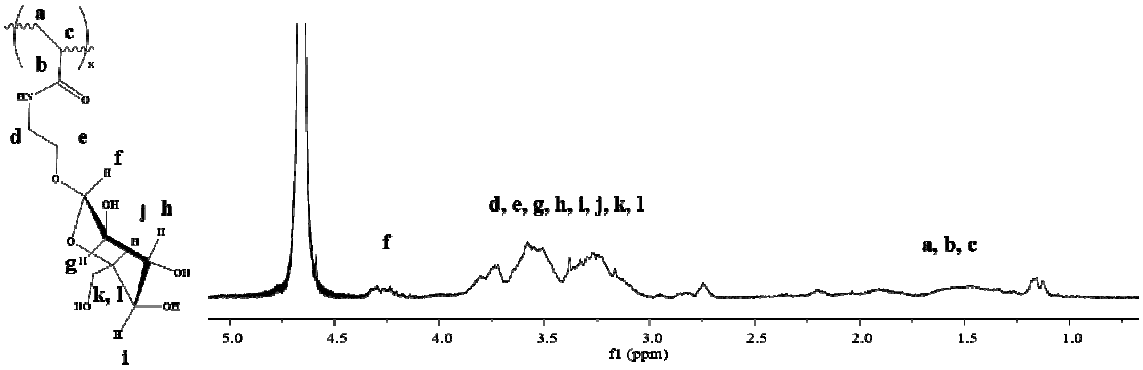

Figure 10. Representative ^{1}H NMR, in deuterated water, of $PGlc_{300}$.

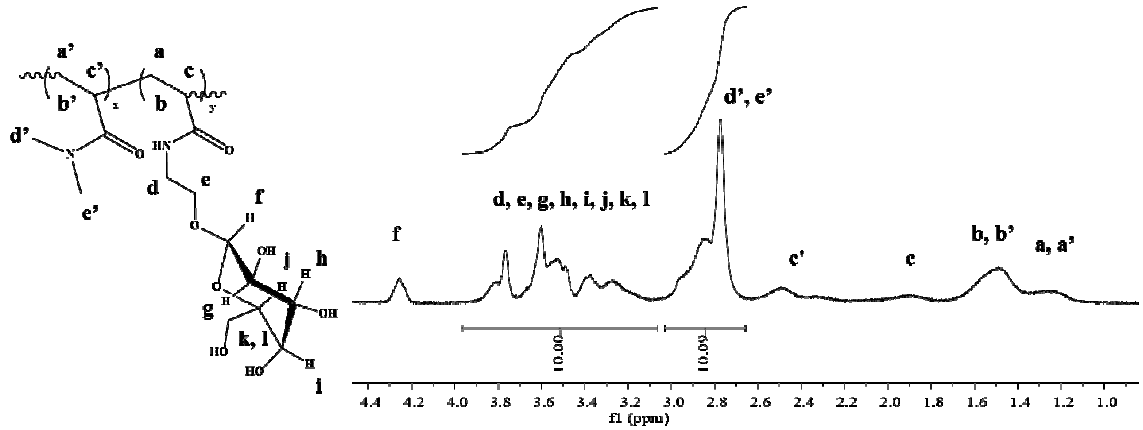

Figure 11. ^{1}H NMR, in deuterated water, of $PDMAGal_{300}$.

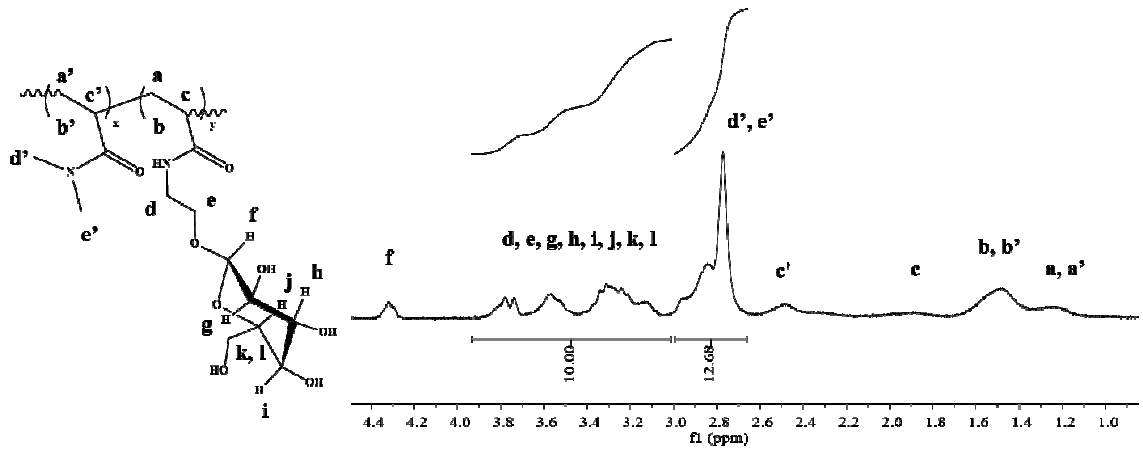

Figure 12. ^{1}H NMR, in deuterated water, of $PDMAGlc_{300}$.

The controlled nature of the polymerization of the homopolymers and copolymers was confirmed through the linear, pseudo first order increase of ln(Mo/M) as a function of time (Figure 13), where Mo is the initial concentration of monomer and M is the monomer concentration at any given time point. An initialization period was seen for all polymers (90 minutes for PGal30 and PGlc30, 30 minutes for PGal300 and PGlc300, and 15 minutes for PDMAGal300 and PDMAGlc300). Researchers attribute this initialization period to the time in which it takes for every CTA molecule to relinquish its R group and add a monomer unit. This is not uncommon with less stable acrylamide radicals, as the CTA prefers to continue interacting with its more stable R group.[22] As a result, a shorter inhibition period is observed for higher monomer to CTA ratios, as there are fewer CTAs that must add monomer. DMA, appears to be a more stable radical than GalEAm and GlcEAm, adds more quickly to the CTA, resulting in a shorter initialization period for the copolymers.

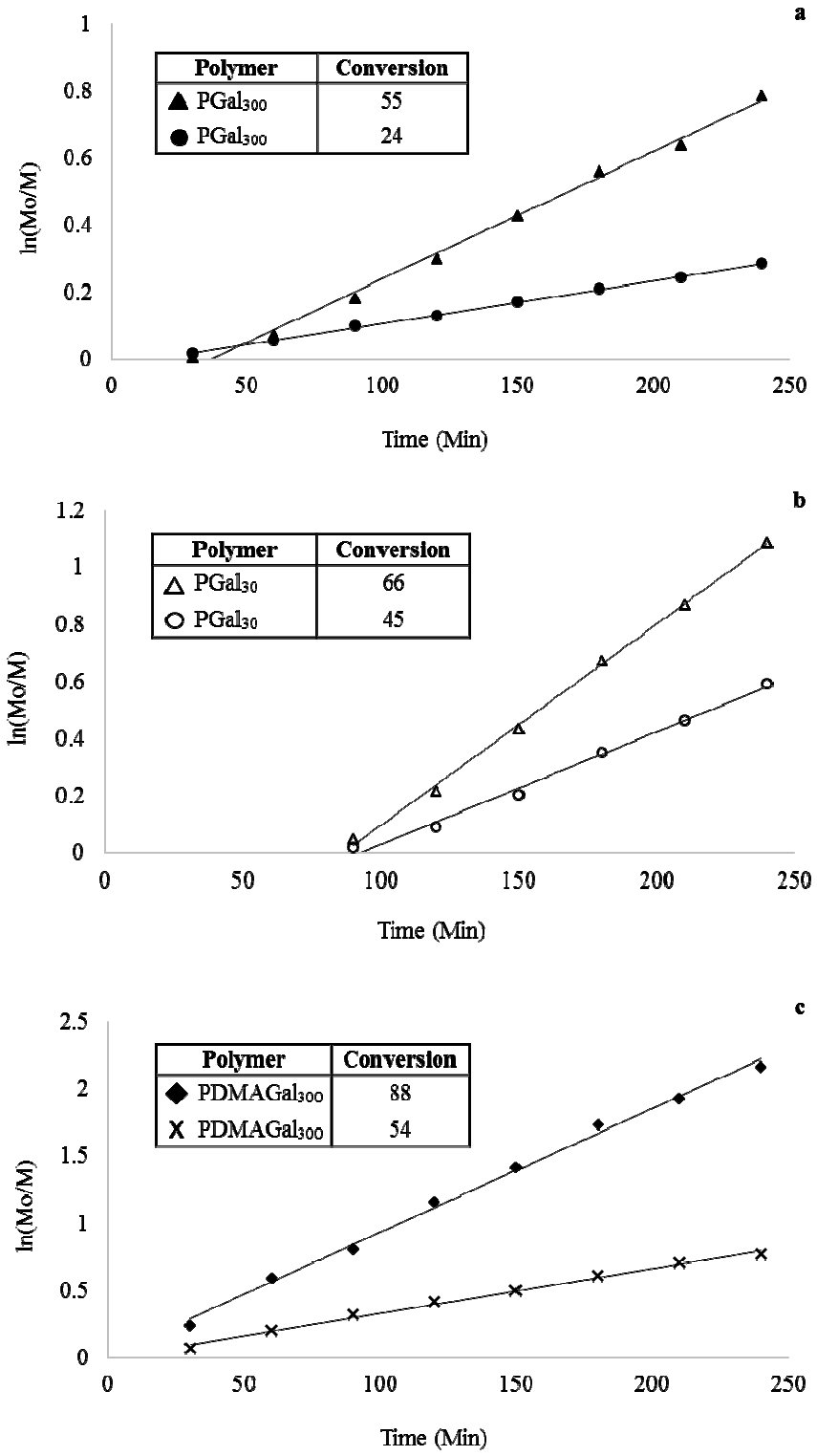

Figure 13. Kinetic plot of ln([M_0]/[M]) as a function of time for a) $PGal_{300}$, $PGlc_{300}$, b) $PGal_{30}$, $PGlc_{30}$ and c) $PDMAGal_{300}$, $PDMAGlc_{300}$. The linear relationship indicated that the polymerization followed a predictable controlled behavior.

Additionally, the rate of polymerization varied between the high and low MW homopolymers, the copolymers and the type of sugar monomer present in each polymer, as seen in *Figure 13a-c*. Across all MWs and polymer compositions, the rate of reaction was faster for polymers with GalEAm, as opposed to GlcEAm. It is currently not understood why monomers that differ at only one stereocenter (C4') would display different reaction rates. The rate of reaction was also faster for the lower molecular weight polymers (PGal30 and PGlc30), as compared to the higher molecular weight polymers (PGal300 and PGlc300). This is attributed to the greater number of radicals present in the lower molecular weight systems.[23] Statistical copolymerization of DMA with GalEAm and GlcEAm resulted in an increase in the rate of polymerization as compared to both MWs of sugar homopolymers.

Evaluation of Aβ aggregation in the presence of glycopolymers

Aβ aggregation was evaluated by ThT fluorescence and SDS-PAGE. In *Figure 14*, ThT fluorescence emission spectra as a function of incubation time for Aβ monomer incubated alone (control) and with DP 300 and DP 30 galactose and glucose glycopolymers, respectively, is shown. An increase in intensity indicates the presence of hydrophobic association of ThT with the molecules. For the Aβ control sample, a characteristic sigmoidal curve is exhibited, which is associated with formation of oligomers that associate to eventually form fibrillar structures. The lag time, or the time before increase in fluorescence associated with aggregation is observed, was shorter for DP 300 PGal than for the Aβ control, showing increased ThT fluorescence at 24 hrs. PGal and PGlc, with DP 30, and $PGlc_{300}$ increase the lag time of aggregation to 72 hours. For the high molecular weight $PGal_{300}$ and $PGlc_{300}$ glycopolymers, fluorescence intensity

plateaus at around 3 a.u. and 1.5 a.u. after 24 and 72hrs, respectively, suggesting that a stabilized aggregate species is formed. Notably, the $PGlc_{300}$ sample dramatically increases the lag time, indicating a uniquely different association pathway for this system. ThT fluorescence for the $PGal_{30}$ solutions does not appear to be statistically different from that of the control, while that of $PGlc_{30}$ solutions is dramatically slower and does not reach the level of the control solution until the final testing point at 144 hours. This indicates that the presence of glucose glycopolymers alters the aggregation pathway. At the final testing point of 144 hours, the low molecular weight glycopolymer solutions and the control show similar levels of fluorescence, indicating the presence of highly aggregated species. The high molecular weight glycopolymer solutions, however, show constant low fluorescence levels indicative of a different type of aggregation.

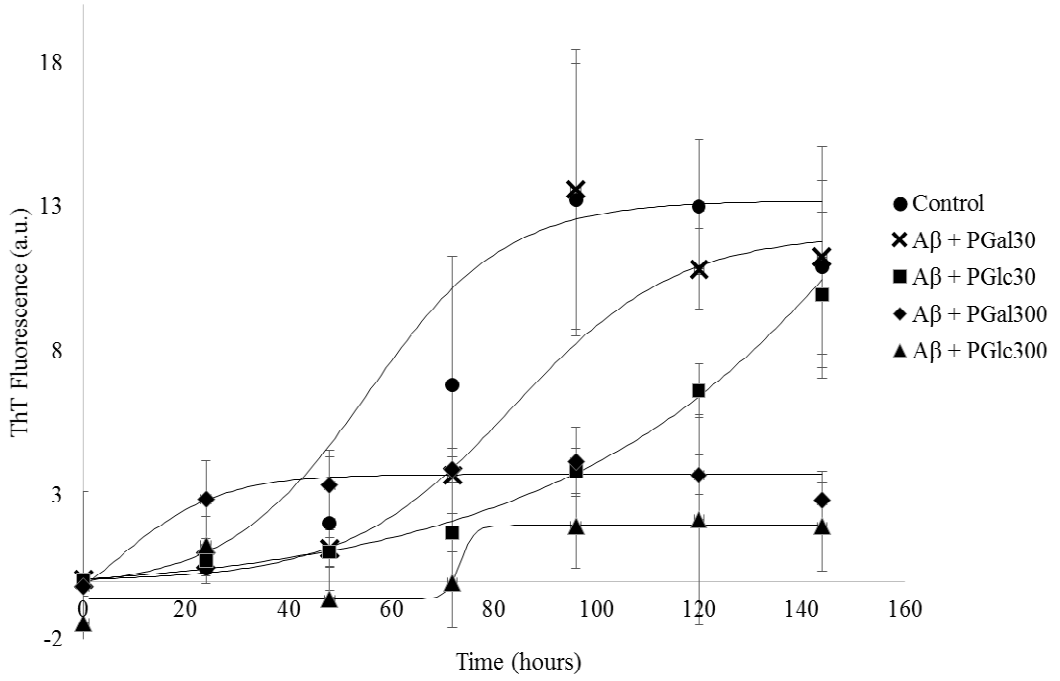

Figure 14. ThT fluorescence emission intensity as a function of time for $PGal_{300}$, $PGal_{30}$, $PGlc_{300}$, and $PGlc_{30}$ with Aβ 42, at a ratio of 1:3 (Aβ:polymer).

SDS-PAGE analysis was performed at 72 and 144 hours of incubation (*Figure 15*). The lane furthest to the left, labelled monomer control, shows a single band at around 3.5 kDA after 72 hours and no band after 144 hours, indicating that in the absence of glycopolymer the Aβ exists in the monomer or highly aggregated state (MW too large to enter the gel). The $PGal_{30}$ and $PGlc_{30}$ lanes show bands at 3.5 kDA and light stains around 200 kDA at 72 hours of incubation, indicating that the Aβ in these solutions exist as monomers or high MW oligomers. At 144 hours of incubation, the monomer band is lighter and the 200 kDA oligomer band is more clearly seen. The Aβ solutions incubated with $PGal_{300}$, at both time points, show bands at 3.5 and 13 kDA, and a diffuse, heavy band at 50-200 kDA, indicating the presence of monomer, low molecular weight oligomers, and high molecular weight oligomers of 11-44mer Aβ units that do not proceed to form fibrils within the tested period. Aβ solutions incubated with $PGlc_{300}$, however, show heavier bands at 13-18 kDA, which correlate to 3-4mer Aβ units, as well heavy diffuse bands corresponding 11-44mers from 50 – 200 kDA. For the $PGlc_{300}$ the monomeric Aβ is not present at 72hrs, in contrast to the other environments tested, indicating that $PGlc_{300}$ quickly causes the formation of oligomers. This is significant as the smaller 3-4mer Aβ units are thought to be the most toxic form of Aβ.[5, 20]

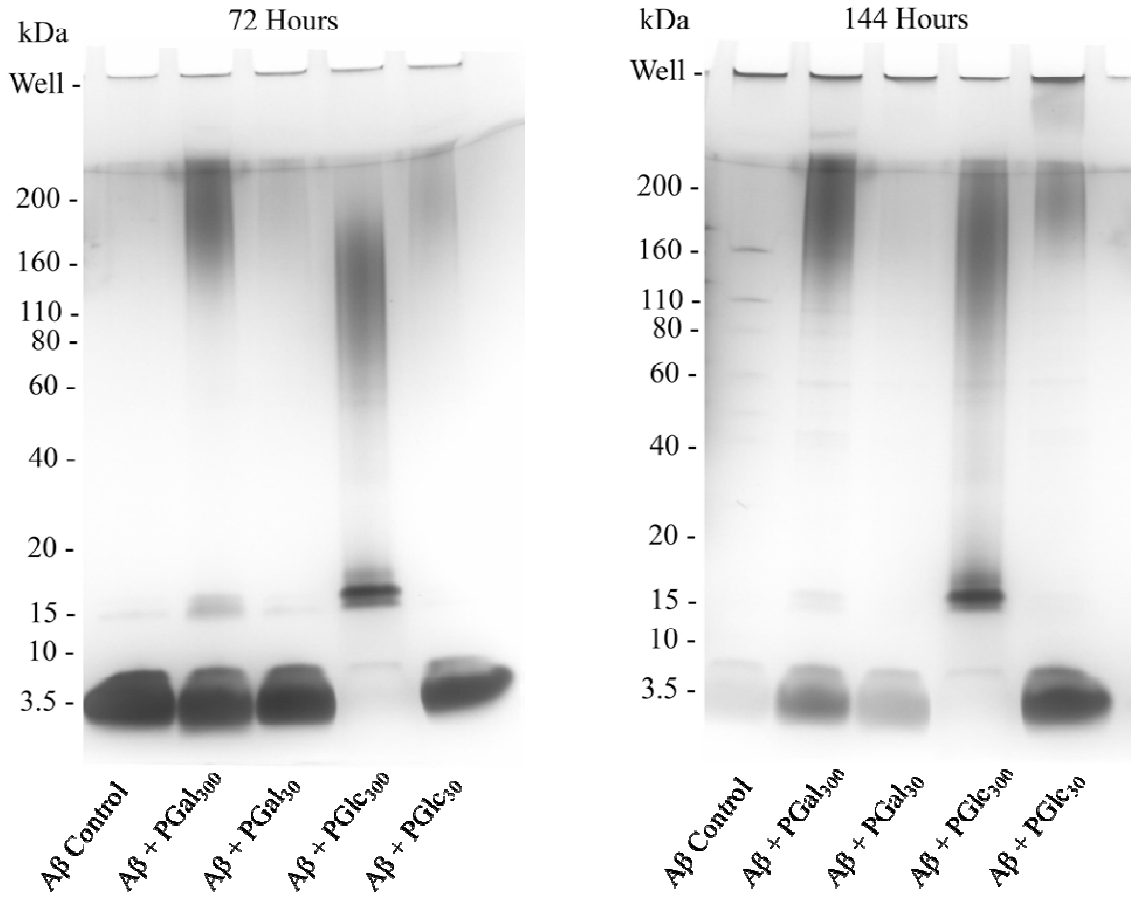

Figure 15. SDS-PAGE of Aβ aggregates that resulted from incubation with glucose and galactose glycopolymers of DP 30 and 300. Glycopolymers are not affected by silver stain and do not appear on the gels.

These results confirm that galactose- and glucose-containing glycopolymers directly influence the aggregation of Aβ, and provide an indication of the expected effects of gangliosides on Aβ aggregation. Both systems promote the formation of large oligomeric aggregates that resemble proto-fibrils, while glucose also promotes the formation of smaller toxic oligomers.

Chapter Summary

Glucose and galactose glycomonomers, with an acrylamide backbone, were synthesized, maintaining control over the stereochemistry at the C1' carbon. They were

polymerized with DMA via aqueous RAFT to produce homopolymers and copolymers of precise molecular weights. Interestingly, different reaction kinetics were observed for the two sugar monomers, GalEAm and GlcEAm, as well as for the various homopolymers and copolymers. Specifically, GalEAm reacts much faster than GlcEAm and the lower MW polymers react faster than the higher MW polymers. Aggregation kinetics and aggregate size of Aβ in the presence of high and low MW glycopolymers were evaluated. Aβ incubated with the $PGal_{300}$ and $PGlc_{300}$ remained at aggregation sizes attributable to oligomers, with $PGlc_{300}$ promoting smaller oligomers (3-4mer) that are potentially more toxic. $PGal_{300}$ also reduced the time required for initial aggregation (lag time). Glucose and galactose glycopolymers with DP 30 increased the lag time of aggregation but ultimately do not impede fibril formation. We report a new platform for synthesis of glycopolymers of controlled architecture which can accommodate a range of biologically relevant saccharides for evaluation of Aβ aggregation pathways in the presence of polysaccharide interfaces.

Recommendation for Future Work

Isolation of oligomeric species, resulting from incubation of Aβ monomer with $PGlc_{300}$, would be an important next step in this project. This would allow for determination of the stability of the oligomeric species, identifying if the aggregation process is "on" or "off" pathway, as described by Kumar *et al.*[20] Additionally, it would allow for conformational analysis of each oligomeric species through circular dichroism (CD). It is currently assumed that the aggregates have formed β-sheets; however, CD must be done to confirm.

The control provided by RAFT polymerization of acrylamide based glycopolymers could also allow for the investigation of other saccharides, such as N-acetyl-D-galactosamine, that are present in GM1 gangliosides, as an incomplete understanding of the GM1 ganglioside head group has been obtained. An alternative monomer synthesis would need to be utilized. Namely, β-alanine would be reacted with acyl chloride, under anhydrous conditions, in order to synthesize an acrylamide monomer with a pendant carboxylic acid. Subsequently, N-acetyl-D-galactosamine, using *N,N'*-dicyclohexylcarbodiimide coupling, could be added to the pendant carboxylic acid. aRAFT polymerization, using the previously described conditions, could then be done to obtain multiple MWs of the galactosamine monomer, which would then allow for a comparative study of Aβ aggregation.

CHAPTER IV

ANTIMICROBIAL PEPTIDE MIMICS AND BACTERIAL INTERFACE

Chapter Overview

This chapter aims to inform the reader of pertinent literature pertaining to antimicrobial peptides and antimicrobial peptide mimics, providing the argument and need for the research presented in Chapter V. Specifically, naturally occurring antimicrobial peptides (AMPs) display the ability to eliminate a wide variety of bacteria, without toxicity to the host eukaryotic cells. Synthetic polymers containing moieties mimicking lysine and arginine components found in AMPs have been reported to show effectiveness against specific bacteria, with the mechanism of activity purported to depend on the nature of the amino acid mimic. In an attempt to incorporate the antimicrobial activity of multiple amino acids in a single water soluble copolymer, a series of copolymers containing lysine mimicking aminopropyl methacrylamide (APMA) and arginine mimicking guanadinopropyl methacrylamide (GPMA) were prepared via aqueous RAFT polymerization. Copolymers were prepared with varying ratios of the comonomers, with degree of polymerization of 30 and narrow molecular weight distribution to simulate naturally occurring AMPs. Antimicrobial activity against Gram negative and Gram positive bacteria, and selectivity via hemolysis of red blood cells and MTT assays of MCF-7 cells, were determined. It was found that broad spectrum antimicrobial effectiveness, including *Pseudomonas aeruginosa*, was obtained for polymers with high levels of APMA, with low toxicity toward eukaryotic cells.

Important Literature

Antimicrobial peptides (AMPs) are naturally occurring defensive agents that eliminate a wide range of bacteria and are found in a variety of eukaryotic organisms, including mammals, insects, and plants. Over 500 unique AMPs are catalogued.[24] Researchers believe that specific environmental needs influence the composition of AMPs. However, these peptides display several consistent characteristics, including a composition of 20-50 amino acid residues, distinct hydrophobic and hydrophilic regions, and a net positive charge at physiological pH (7.4). The hydrophilic regions have an abundance of lysine and arginine amino acid residues, which are protonated and positively charged under physiological conditions. It is this net positive charge that enables AMPs to selectively bind to bacteria, as their membranes are negatively charged, and induce cell death. The host eukaryotic cells have a net neutral charge and, therefore, do not have as high an affinity for AMPs, resulting in an efficient and selective defense against bacteria.

AMPS are of interest because bacteria do not appear to develop resistance to AMP activity as readily as they do against current synthetic antibiotics. Unfortunately, isolation or synthesis of sufficient quantities of AMPs is difficult and costly. Polymeric mimics of AMPs are a desirable alternative because they have the potential to be produced at reduced cost and are easier to synthesize.[25]

Several parameters are known to affect the efficacy of successful AMP mimics. First, polymers of lower molecular weight, around that of natural AMPs, show greater antimicrobial activity than monomers or higher molecular weight systems.[26] Second, the amphipathic balance of the polymer mimic is essential for optimal antibacterial activity

as well as selectivity. Polymeric AMPs that are too hydrophobic reduce selectivity and result in eukaryotic cell death. A number of different methods have been employed to modify the amphipathic balance in synthetic systems. Researchers increased hydrophobicity through copolymerization of hydrophobic monomers with alkyl tails of different lengths with cationic comonomers, which generally resulted in increased bacterial cell death at the expense of selectivity.[27] Multiple polymer backbone structures, including methacrylates,[27a, 27b, 28] β-lactams,[29] norbornenes,[30] and methacrylamides[27c, 31] with varying solubility and inherent polarity have been evaluated as AMP mimics. Palermo *et al.* showed that methacrylamide based AMP mimics, due to the increased polarity of the amide, had a decreased toxic impact on red blood cells as compared to similar methacrylate based polymers. [27c, 28a] These methacrylamide polymers also demonstrated increased antimicrobial activity, as the more soluble backbone allowed complete protonation, and, therefore, increased charge density, of the primary amine cationic moiety.

The choice of cationic moiety also impacts the effectiveness of synthetic AMP mimics. Mostly primary amines,[27b, 29-30, 31] which mimic lysine amino acid residues, have been employed; however, tertiary[31] and quaternary[28a] amines have also been investigated. Results indicate, however, that transition from primary to tertiary or quaternary amines reduces activity and selectivity of AMPs. In our previous work, we investigated the effect of pendant cation modification with various alkyl groups to alter the amphipathic ratio of methacrylamide AMPs, and found that unmodified primary amine cations display superior antimicrobial activity and selectivity.[31] Researchers have also begun to explore guanidinium, which mimics arginine amino acid residues found in

natural AMPs, as an alternative cationic moiety. Gabriel *et al.*, using a polynorbornene backbone, reported that substituting guanidinium for primary amines improved selectivity without affecting the antimicrobial activity.[30b] Locock *et al.*, using a methacrylate backbone, reported that guanidinium improved both activity and selectivity.[28b]

Naturally occurring AMPs demonstrate different mechanisms of bacterial cell death based on the prevalence of lysine or arginine in the peptide. The two principal mechanisms are (1) cell penetration, which correlates with a predominance of arginine, and (2) membrane disruption, which correlates with an increased occurrence of lysine.[24, 32] Similarly, guanidinium based AMP mimics appear to kill bacterial cells in a manner that differs from that of primary amine based AMP mimics. Specifically, guanidinium functionalized polynorbornenes did not demonstrate the bacterial membrane disruption behavior observed in primary amine functionalized polynorbornenes, suggesting that cell death proceeded via an alternate mechanism.[33] Locock and coworkers reported that increasing the molecular weight of their guanidinium AMP mimics resulted in reduced antimicrobial activity, while the antibacterial effectiveness of primary amine AMP mimics was less sensitive to changes in molecular weight over the range tested. These findings suggest the possibility of improving antimicrobial properties by incorporating both lysine and arginine mimics in synthetic AMPS, which should provide the ability to kill bacteria through different mechanisms and be effective against a wider selection of bacteria.

Treat and coworkers investigated the viability of poly(3-guanidinopropyl methylacrylamide) copolymers as cell penetrating vehicles for potential drug delivery applications. They found that significant amounts of polymer were taken into the

eukaryotic KB cell through endocytotic and passive pathways.[34] These results indicate the potential reduction in selectivity for guanidinium-containing AMP mimics, and suggest the need for further study of the effectiveness of the systems. Investigation into the effect of counterion type on antimicrobial activity is also needed.[35] Previous reports have separately employed TFA or Cl counterions with gauanidinium moieties; however, to our knowledge, the effects of counterion structure have not been reported.[28b, 30b]

Antimicrobial activity of AMP mimics has been tested against both gram-positive bacteria, which have a cell wall that surrounds an inner plasma membrane, and gram-negative bacteria, which have a thin cell wall that is sandwiched between two plasma membrane layers. Typically, *E. coli*, Gram-negative, and *B. subtilis*, Gram positive, are used as representative bacteria in antimicrobial activity testing. However, to our knowledge, the effects of synthetic AMPs on *Pseudomonas aeruginosa*, which displays an inordinate ability to resist traditional therapeutics and is the most reported nosocomial bacterium,[36] have not yet been evaluated. *Staphylococcus aureus*, due to the emergence of methicillin resistant strains, is also of great concern.

In this study, statistical copolymers of aminopropyl methacrylamide (APMA) and 3-guanadinopropyl methacrylamide (GPMA) of controlled molecular weight and composition are prepared via aqueous RAFT polymerization for determination of the effects of lysine- and arginine-mimicking pendant groups in a fully water-soluble AMP mimic on antimicrobial activity and selectivity. Polymers are prepared with molecular weights similar to those of naturally occurring AMPS, and the effects of counterion type are examined. The low molecular weights of the synthesized polymers eliminate the need for built-in biodegradability, as small molecules are removed from the body via the

renal system.[37] Under the benign aqueous RAFT reaction conditions, Boc-protection of the amine-containing monomers is not required.

Antimicrobial behavior against *E. coli*, *S. aureus*, and *P. aeruginosa,* and selectivity testing via hemolysis of red blood cells and MTT assays of MCF-7 cells are reported. Broad spectrum antimicrobial effectiveness coupled with low toxicity towards eukaryotic cells is observed for copolymers with high concentrations of the lysine-mimicking APMA monomer.

CHAPTER V

EXPERIMENTAL DETAIL FOR ANTIMICROBIAL PEPTIDE POLYMER MIMICS

Research Overview

Our ultimate goal is to investigate the effectiveness of guanidiniums moieties within our established methacrylamide based platform for AMP mimic development and tailoring via tuning of (co)polymer composition. Attachment of guanidinium has previously resulted in improved activity and selectivity of AMP mimics.[28b, 30b] This research aims to increase antimicrobial activity and selectiveness across a broader spectrum of bacteria through pairing of increased solubility of a methacrylamide polymer backbone and guanidinium pendant groups. In this chapter, we describe a novel method for GPMA synthesis that allows for improved yield, simplified purification and handling. Additionally, a range of GPMA-stat-APMA copolymers were synthesized for the first time using aqueous RAFT polymerization, which allows for control over MW, narrow PDI and benign reaction conditions. Polymerization, due to the benign reaction conditions, did not require Boc-protection of APMA or GPMA. Antimicrobial behavior against E. *coli*, S. *aureus*, and *P. aeruginosa*, which to the best knowledge of the author has never been reported in polymeric AMP papers, was performed, and selectivity testing via hemolysis of red blood cells and MTT assays of MCF-7 cells was done. As before, the low molecular weights of synthesized polymers eliminates the need for built in biodegradability, as small molecules can be removed from the body via the renal system.[37]

Objectives of Research and Research Questions

I. Synthesize statistical copolymers of APMA and GPMA via aqueous RAFT polymerization to expand upon our previous polymeric AMP platform and enable a systematic evaluation of the effect of pendant guanidinium cations.
   a. *Is APMA and GPMA able to be statistically synthesized via aqueous RAFT polymerization?*

II. Determine the antimicrobial activity and selectivity of synthetic AMP mimics as a function of the polymer guanidinium content and counterion identity.
   a. *Does the addition of guanidinium increase the antimicrobial activity of synthesized AMPs over a broader range of bacteria?*
   b. *Is there indication of an alternative bacterial death mechanism with the incorporation of guanidinium?*

Materials and Methods

Materials

For GPMA synthesis, N-(3-aminopropyl) methacrylamide hydrochloride, >98% (APMA·HCl) (Polysciences, Inc.), triethylamine, >99.8% (TEA) (Sigma-Aldrich, USA), N, N'-di-boc-1H-pyrazole-1-carboxamidine (PCA) (Sigma-Aldrich, USA), acetonitrile, anhydrous, 98% (Sigma-Aldrich, USA), sodium sulfate (Sigma-Aldrich, USA), trifluoroacetic acid (TFA) Sigma-Aldrich, USA) and 4M HCl in dioxane (Fischer Scientific, USA) were used as purchased. For all polymerizations, 4, 4'-Azobis (4-cyanopentanoic acid) (V-501) (Sigma-Aldrich, USA), methanol, anhydrous, 99.8% (Fischer Scientific, USA), sodium acetate, anhydrous (Sigma-Aldrich, USA), acetic acid, glacial (Fisher Scientific, USA) and Spectra/Por® dialysis membrane, standard RC

tubing (3,500 kD) (Spectrum Laboratories, Inc., were used as purchased. 4-cyano-4-(ethylsulfanylthiocarbonylsulfanyl)pentanoic acid (CEP) was used as the CTA in all polymerizations and was synthesized via previously published procedures.[18] For antimicrobial susceptibility testing, *Escherichia coli* (ATCC), *Staphylococcus aureus* (ATCC), *Pseudomonas aeruginosa* (ATCC), Mueller-Hinton broth (MHB) (Fischer Scientific) and low salt Luria Broth (10 g/L tryptone, 5g/L yeast extract, 0.5 g/L NaCl) (LB) (Sigma-Aldrich, USA) were used as purchased. Tris (hydroxymethyl) aminomethane (Tris) (Sigma-Aldrich, USA) and NaCl (Sigma-Aldrich, USA) were used to make tris-buffered saline (TBS) (10 mM Tris, 150 mM NaCl, pH 7.4). All selectivity testing was done with Triton-X 100 (Merck, India), Dulbecco's Modified Eagle Media (DMEM) (Himedia, India), fetal bovine serum (FBS) (Himedia, India), Trypsin-EDTA Solution 1X (Himedia, India), antibiotic solution 100X Liquid (AS) (made with penicillin and streptomycin) (Himedia, India), (3-(4,5-dimethylthiazol-2-yl)-2,5-diphenyltetrazolium bromide (MTT) (Sigma-Aldrich, India) and dimethyl sulfoxide (DMSO) (Merck, India), and used as received. Preparation of MCF-7 cells (NCCS, Pune, India) is discussed in the cell viability section of this paper. Isolation of red blood cells (RBC) (AIIMS hospital, New Delhi, India) is discussed in the hemolysis section of this paper.

Synthesis of Boc-protected GPMA

APMA·HCl, dissolved in a mixture of DI water (12 mL) and TEA (20 mL, 148 mmol), was stirred at 25°C. PCA (10 g, 32 mmol), dissolved in acetonitrile (108 mL), was then added drop-wise, over 30 minutes, to the stirring APMA·HCl solution via an addition funnel (*Scheme 4*). The reaction progressed for 24 hr. The product was purified

via filtration, washed three times with DI water (50 mL) and lyophilized overnight (yield: 91%). ^{1}H NMR (300 MHz, CDCl3): δ [ppm] 1.46 and 1.50 (d, H-G); 1.70 (m, H-D); 2.00 (s, H-C); 3.32 (m, H-F); 3.49 (m, H-E); 5.31 (s, H-A); 5.81 (s, H-B); 7.39 (t, H-H); 8.49 (t, H-I); 11.53 (s, H-J).

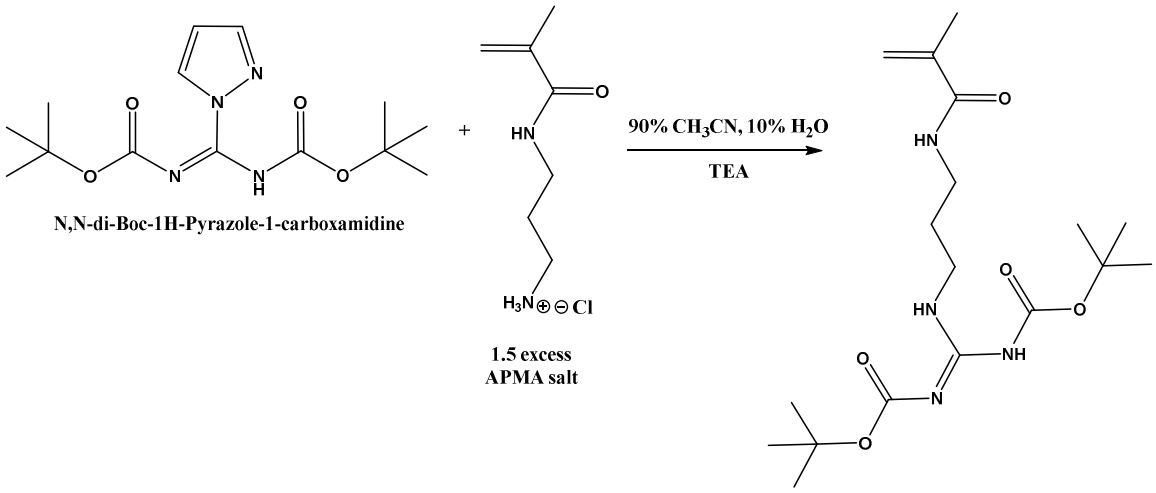

Scheme 4. Synthesis of Boc-protected GPMA.

Deprotection of Boc-protected GPMA

Deprotection of GPMA proceeded in one of two ways in order to alter the counterion coordinated to the guanidinium, as the conjugate base of the acid used to deprotect becomes the counterion. First, Boc-protected GPMA (10.96 g, 28.48 mmol) was dissolved in CH_2Cl_2 (90 mL), stirring at 0°C. TFA (87 mL, 1.14 mol) (20 eq. per boc-protecting group) was then added to the solution drop-wise via an addition funnel and the reaction was allowed to progress for 16 hours, while gradually warming from 0°C to 25°C (*Scheme 5*). The solvents were removed via rotary evaporation and the resulting clear viscous oil was dissolved in 250 mL DI H_2O, frozen in liquid N_2, and lyophilized for 48 hr. The product was obtained as a white solid. Second, Boc-protected GPMA was dissolved in 4M HCl in dioxane (7 eq. per boc-protecting group) and allowed to react

overnight. The product, a white solid, precipitated from solution and was purified via filtration and washing with anhydrous dioxane. ^{1}H NMR (300 MHz, DMSO): δ [ppm] 1.65 (m, H-D'), 1.86 (s, H-C'), 3.13 (m, H-E', F'); 5.34 (s, H-A'); 5.66 (s, H-B'); 7.27 (s, broad, H-H', I'); 7.70 (t, H-J'); 8.00 (t, H-K').

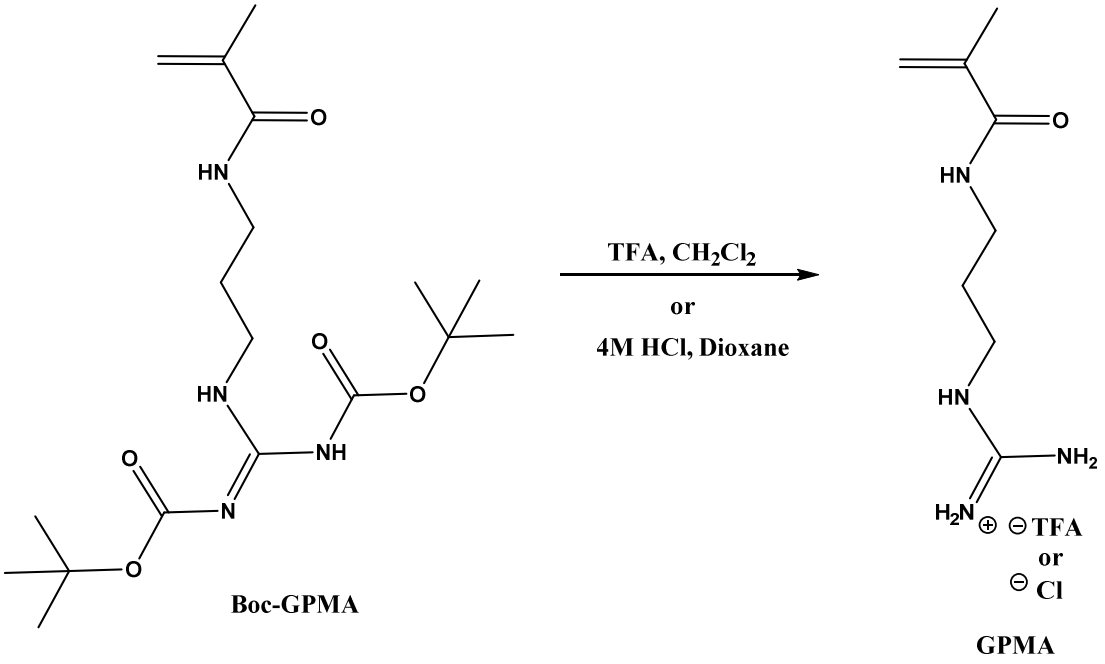

Scheme 5. Deprotection of Boc-protected GPMA with either TFA or HCl, which alters the resulting counterion for deprotected GPMA.

Polymerization of Antimicrobial Peptide (AMP) Mimics

Utilizing aqueous RAFT polymerization, polymer molecular weights were targeted by selecting appropriate initial monomer and CTA concentrations. The ratio of M_0:CTA_0 was set to be approximately 30:1 to yield a degree of polymerization of ~30, which mimics the size of naturally occurring AMPs. 4, 4'-Azobis (4-cyanopentanoic acid) was used as the initiator. For all polymerizations, CTA_0/I_0=5. The polymerization was conducted in aqueous acetate buffer (1.5 M sodium acetate and 0.5 M acetic acid, pH 5) at 70°C[19] for 6 hr (*Scheme 6*). Methanol was added in low quantities (~30%) to

improve the solubility of CEP in the aqueous media. After the reactions were completed the solutions were exposed to air and quenched in liquid nitrogen. The solutions were then dialyzed against water for 72 hours, lyophilized for 72 hours, and then stored in desiccant until subsequent testing (representative yield: 75%). Some polymer was lost in dialysis due to excessive swelling of the dialysis tubing as a result of internal osmotic pressure. This loss can be minimized by making the water slightly acidic during the dialysis procedure to reduce the extent of swelling.

The mol % of GPMA was varied to produce nine homo- and co-polymers. The nomenclature PGT represents polyGPMA and the corresponding number indicates the targeted mole fraction in the (co)polymer. For example, PGT25 represents a copolymer composed of 25 mol% GPMA·TFA and 75 mol% APMA·Cl. The addition of either ·Cl or ·TFA indicates which counterion was coordinated with GPMA when it was polymerized.

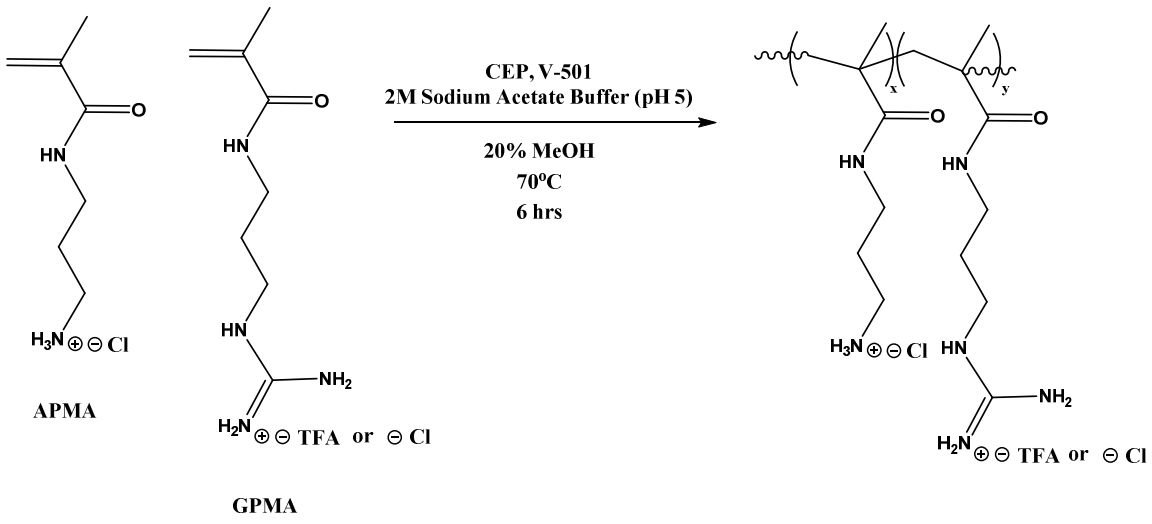

Scheme 6. Aqueous RAFT polymerization of poly(APMA-*stat*-GPMA) with either TFA or Cl as the counterion for GPMA.

Nuclear Magnetic Resonance (NMR)

^{1}H NMR was performed with a Varian Mercury^{PLUS} 300 MHz spectrometer in $CDCl_3$ and DMSO, utilizing delay times of 5 s to determine monomer purity. A 500 MHz NMR equipped with a standard 5 mm ^{1}H/^{13}C probe and operating at 499.77 MHz (^{1}H) was used to identify the structures of PAPMA and PGPMA homopolymers and the structures of the poly(APMA-*stat*-GPMA) copolymers, with counterions of $^{-}$TFA and $^{-}$Cl, in D_2O. 64 scans were taken for each experiment with a 3.1 second recycle delay. For each of the homopolymers, unique peak assignments were made, and the copolymer compositions were calculated for the statistical polymers via peak integration of methylene bridge E and E' on the APMA and GPMA monomer residues, respectively.

The polymerization reaction progress was monitored, and the controlled nature of the reaction was ensured for PGT50·TFA through aliquots that were taken every hour from the reaction vial. ^{1}H NMR was utilized to determine [M] at time (t) by comparing the vinylic hydrogen peak integrations to the integration of an internal standard (MeOH).

Aqueous Size Exclusion Chromatography

The molecular weight and polydispersity index (PDI) of the polymers were determined by aqueous size exclusion chromatography (ASEC) coupled with multi-angle laser light scattering (MALLS). Eprogen CATSEC columns (100, 300 and 1000 Å) were used in combination with a Wyatt Optilab DSP interferometric refractometer (k = 690 nm) and a Wyatt DAWN DSP MALLS detector (k = 633 nm). 1 wt% acetic acid/ 0.1 M Na_2SO_4 (aq) was used as the eluent at a flow rate of 0.25 mL/min. The interferometric refractometer was utilized off-line to determine dn/dc values for PAPMA and PGPMA at 25 °C in the eluent (1 wt% acetic acid/ 0.1 M Na_2SO_4 (aq)) in order to assign absolute

molecular weight values to all homopolymers. For the statistical polymers the dn/dc values were calculated as the mole-fraction-averaged composites of the measured homopolymer dn/dc values using the copolymer compositions determined by ^{1}H NMR. Wyatt ASTRA SEC/LS software was used for molecular weight and PDI calculations. ASEC-MALLS was also utilized to monitor molecular weight as a function of time. The refractive index (RI) response vs elution volume, for aliquots taken at each time interval, was collected.

Antimicrobial Susceptibility Assay

Antimicrobial susceptibility was measured using the broth microdilution method according to the CLSI guidelines.[38] Bacterial strains were incubated in MHB and all measurements were performed in triplicate. Two-fold serial dilutions of each antimicrobial peptide mimic solution (1000 μg to 15.6 μg /ml) were prepared in a 96 well Costar® microtiter plate. The microtiter wells were then inoculated with 5×10^5 colony forming units per ml of each test strain.[39] After overnight incubation at 37°C, wells were analyzed for bacterial growth by measuring OD_{580} using a plate reader. MHB without any peptides was also inoculated with each strain and used as a positive control for microbial growth. Sterile MHB was used as a negative control and as a blank for absorbance readings. The lowest concentration (μg/ml) of the peptides that completely prevented bacterial growth was considered the minimum inhibitory concentration (MIC).

Additionally, antimicrobial susceptibility was tested using a procedure developed by Paslay *et al*.[31] Namely, bacteria were grown overnight in low salt LB and then diluted to 0.001 OD_{600}. Polymer solutions, in TBS at concentrations of 70, 150, 230 and 300 μg/mL, respectively, were incubated in a 96 well plate overnight at 37°C, with an equal

volume of the diluted bacterial suspensions. Subsequently, the optical density of each well was measured using a UV-Vis plate reader to determine the level of bacterial growth in comparison to the positive and negative standards.

Hemolysis Assay

Hemolysis testing was done in accordance with the procedure previously published by Paslay *et al.*[31] Whole blood was received from AIIMS hospital in New Delhi, India, requiring processing in order to isolate red blood cells (RBC). The whole blood was centrifuged at 1500 rpm for 10 min, resulting in a RBC plug at the bottom of the centrifuge tube. Undesired serum was decanted, leaving the RBC plug. RBCs (30 µL) taken from the plug were suspended in TBS (10 mL) and then centrifuged at 1500 rpm for 10 min. Suspension in TBS and centrifugation was repeated a total of three times to adequately rinse RBCs. The final RBC solution consisted of rinsed RBCs suspended in TBS (10 mL). Simultaneously, stock solutions at concentrations relevant to determined MICs of all homo- and copolymers were made using TBS.

RBCs and polymers solutions were incubated together in micro-centrifuge tubes at a 1:1 ratio, with a total volume of 1 mL, at 37°C for 30 min. The micro-centrifuge tubes were then centrifuged at 1500 rpm for 10 min to separate the intact, healthy RBCs from the rest of solution. The supernatant, containing hemoglobin released from polymer lysed RBCs, was transferred to a 96-well plate (100 µL in triplicate) where absorbance at 540 nm was determined in a Biotek PowerWave X S2 UV-VIS plate reader. Percent hemolysis was determined through normalization of the observed absorbance for individual polymer wells to that of positive (100% hemolysis) and negative (0% hemolysis) controls.

MTT Assay

Further selectivity testing was performed as previously described against MCF-7 cancer cells. Cells were grown to 80% confluence at 37°C in a 5% CO_2 incubator, using tissue culture polystyrene flacon flasks and DMEM media that was supplemented with 10% fetal calf serum and 1% antibiotic serum.[31] Trypsin was added to dissociate cells from the flacon flask; cells were counted in a hemocytometer to determine cell concentration. Fresh media was then added to the flacon flask so that cells could be seeded into a 96 well plate (100 µL per well). Seeded cells were incubated for 24 hours at 37°C in a 5% CO_2 incubator. The old media was then removed from each well and replaced with fresh media (100 µL per well). Polymer solutions (50 µL per well) were added to appropriate wells in triplicate, resulting in final polymer concentrations of 25, 100, 200, 2000 µg/mL, respectively. TBS (50 µL per well) and 3% Triton-X (50 µL per well) were added, in triplicate, as the positive and negative controls, respectively. Plates were incubated for either 6 or 12 hrs at 37°C in a 5% CO_2 incubator. Old media was then removed and replaced with new media (100 µL per well). MTT in TBS (10 mg/mL, 10 µL per well) was added and allowed to incubate for 4 hrs at 37°C in a 5% CO_2 incubator. Old media was removed and DMSO (100 µL per well) was added to dissolve formazan crystals produced by living MCF-7 cells. Absorbance of each well was read at 570 nm using a Biotek PowerWave X S2 UV-VIS plate reader. Percent cell viability was determined by normalizing the measured absorbance in polymer wells with the absorbance in the positive and negative control wells.

Results and Discussion

GPMA Synthesis and (Co)polymerization

Guanidinium functionalized synthetic AMP mimics were prepared to compare the broad-spectrum antimicrobial effectiveness of arginine and lysine analogues when incorporated as pendant groups into fully water-soluble, hydrolytically stable, methacrylamide copolymers (*Scheme 7*). We previously demonstrated high selectivity and toxicity against *E. coli* (Gram-negative) and *B. subtilis* (Gram-positive) for lysine-mimicking APMA polymers. These findings combined with literature reports of antimicrobial effectiveness obtained with incorporation of guanidinium moieties in other polymeric systems,[28b, 30b] and the McCormick group's previous copolymer reports of GPMA synthesis,[34] provided the motivation for the current study. Methacrylamide based monomers were chosen for their previously demonstrated antimicrobial activity and selectivity, hydrolytic stability, high degree of water solubility, and pKa values (ensuring ionization at physiological pH).

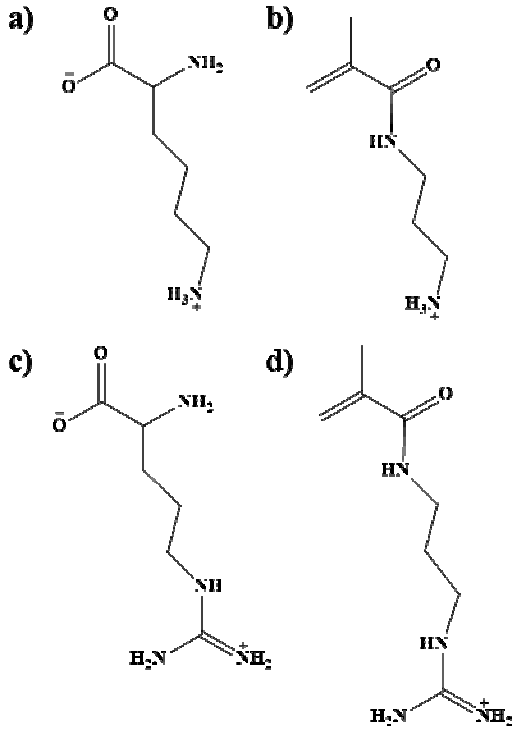

Scheme 7. APMA (b) and GPMA (d) mimics of lysine (a) and arginine (c) amino acid residues, respectively.

Increased monomer purity and yield for GPMA were obtained through modifications of the synthetic methods reported by Treat *et al.*[34] and Gabriel *et al.*[30b] Specifically, APMA·HCl was deprotonated in situ with TEA, allowing nucleophilic attack on the PCA, as shown in *Scheme 4*. The resulting Boc-GPMA precipitated at high yield (~91%) from solution, with byproducts removed through subsequent filtration and washing with DI water. This reaction was more facile than the previous synthesis by Treat *et al*., who reported deacidification of purchased APMA followed by drop-wise addition to a stirring solution of 2-ethyl-2-thiopseudourea and TEA in acetonitrile. Additionally, the reaction required column chromatography for purification and resulted in a 72% yield. In our current procedure, GPMA was deprotected, shown in *Scheme 5*, before polymerization through a well-established Boc-deprotection protocol[30b] with either

TFA or HCl. This allowed production of GPMA monomers at quantitative yield with counterions of different bulkiness and binding affinities.

Table 2

Molecular weight and composition data for GPMA synthesized (co)polymers.

Polymer	mol % GPMA (theory)	mol % GPMA (exp)[a]	$Mn_{,th}$ (g/mol)[b]	$Mn_{,exp}$ (g/mol)[c]	PDI[c]	*dn/dc*[d]
1. (PAPMA·Cl)	0	0	5,600	6,500	1.06	0.200
2. (PGT25·TFA)	25	23	6,500	6,900	1.03	0.183
3. (PGT50·TFA)	50	45	7,400	6,100	1.06	0.169
4. (PGT75·TFA)	75	72	8,300	5,800	1.12	0.152
5. (PGT100·TFA)	100	100	9,200	8,100	1.04	0.132
6. (PGT25·Cl)	25	30	6,500	7,000	1.11	0.183
7. (PGT50·Cl)	50	44	7,400	7,400	1.12	0.169
8. (PGT75·Cl)	75	67	8,300	8,100	1.16	0.152
9. (PGT100·Cl)	100	100	9,200	9,200	1.11	0.132

[a]Determined by ^{1}H NMR. [b]Based on 90% conversion of [M_0]. [c]Determined by ASEC-MALLS. [d]Determined by a Wyatt Optilab DSP interferometric refractometer.

GPMA copolymers of controlled molecular weight, narrow molecular weight distribution, and desired composition were prepared via aqueous RAFT polymerization as described in the experimental section (*Table 2*). Measured values of molecular weight and GPMA incorporation are in good agreement with predicted values. All polymers show narrow molecular weight distributions, with PDIs smaller than 1.2. A plot of $\ln([M_0]/[M])$ for the polymerization of the 1:1 molar ratio of APMA:GPMA·TFA as a function of reaction time is linear (*Figure 16*), indicating pseudo first order kinetics and control of the polymerization. Furthermore, GPC analysis (*Figure 17*) shows a steady

increase in MW and narrowing of MWD as a function of reaction time, suggesting controlled polymerization.

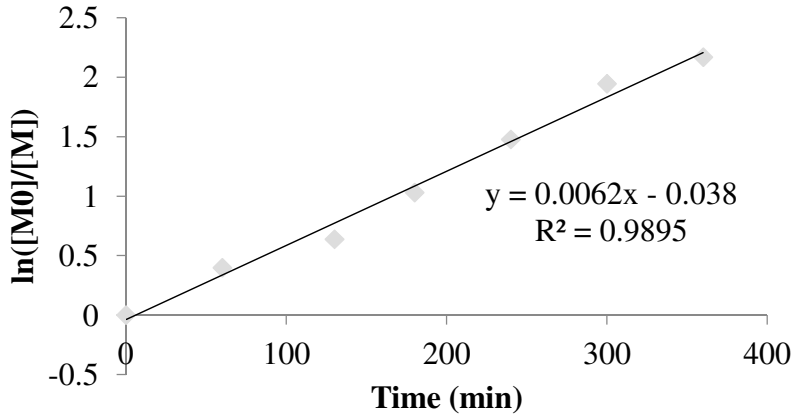

Figure 16. Poly(APMA-*stat*-GPMA) reaction kinetics. Kinetic plot of ln([M_0]/[M]) as a function of time for the polymerization of 1:1 molar ratio of APMA:GPMA·TFA.

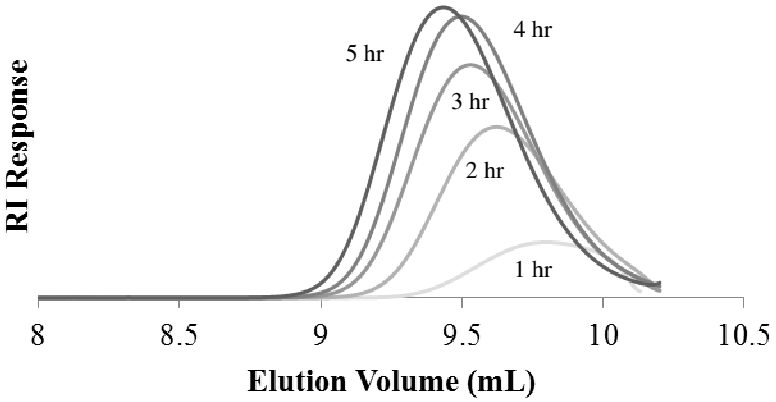

Figure 17. Poly(APMA-*stat*-GPMA) molecular weight distribution and conversion as a function of reaction time for the polymerization of 1:1 molar ratio of APMA:GPMA·TFA.

In a representative ^{1}H NMR spectrum of poly(APMA-*stat*-GPMA) targeted at a 50:50 mole ratio (*Figure 18*), clearly identifiable peaks for the monomer residues of both APMA and GPMA are visible. The methylene bridge carbon nearest the amide, labelled D in *Figure 18*, is attributed to both APMA and GPMA residues. For proper integration,

comparison of protons labelled E (2.8 ppm), from APMA, and E' (3.0 ppm), from GPMA, and removal of proton contribution from D (3.0) are required. Evaluation of the integrated peaks indicates 45 mole % incorporation of GPMA into the copolymer, which is close to the target composition. Similar kinetic plots, GPC traces, and ^{1}H NMR analyses were obtained for all copolymer compositions. It was important to ensure that the targeted MW and copolymer composition were achieved in order to separate the effects of MW and MWD from those of polymer composition and counterion type on antimicrobial activity and selectivity.

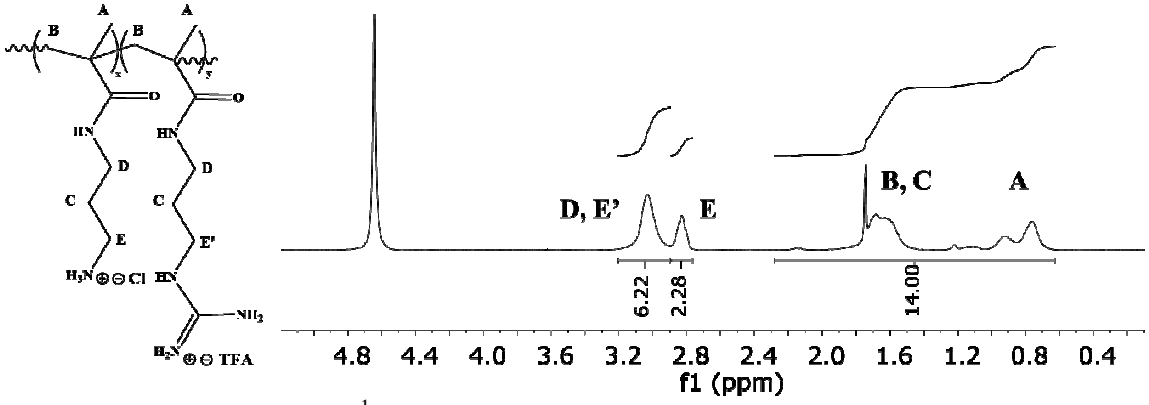

Figure 18. A representative ^{1}H NMR spectrum of poly(APMA-*stat*-GPMA) copolymer (1:1 molar ratio of APMA:GPMA·TFA in feed).

Antimicrobial activity

Broth microdilution testing, as described in the experimental section, was completed to determine the effectiveness of the controlled copolymers as antimicrobial agents. Activity was quantified based on the minimum inhibitory concentration (MIC), which is the polymer concentration at which 100% cell death occurs. Results of the broth microdilution studies are provided in *Figure 19* as plots of UV-Vis absorbance as a function of polymer concentration for each of the copolymer compositions against (a) *S. aureus*, (b) *E. coli*, and (c) *P. aeruginosa*. Lower absorbance indicates higher activity.

For the copolymers providing 100% cell death in the therapeutic range (concentrations ≤ 1000 μg/mL), MIC is tabulated in *Table 3*.

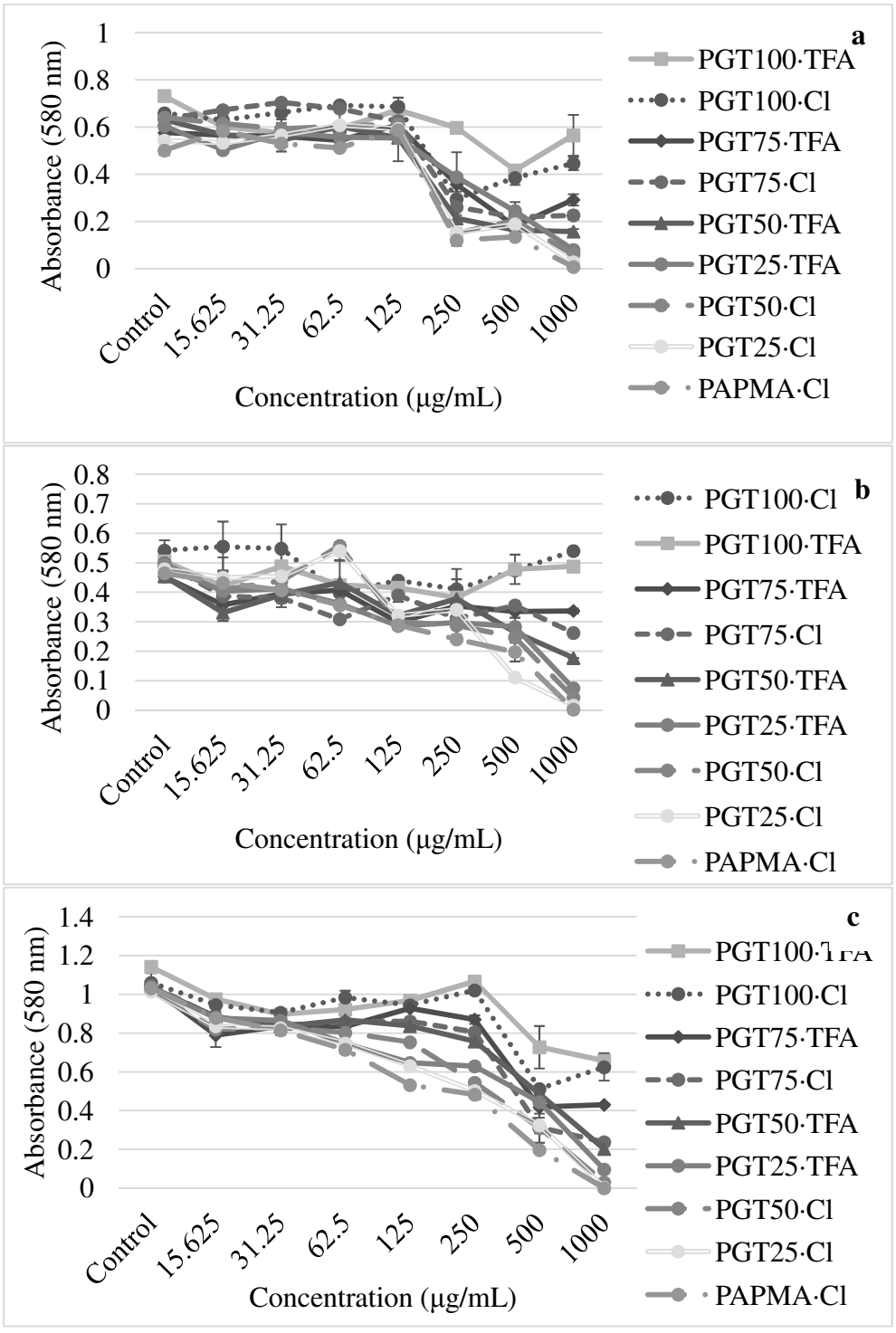

Figure 19. Broth microdilution results for all synthesized AMP mimics against (a) *S. aureus*, (b) *E. coli*, and (c) *P. aeruginosa*, where decreased absorbance correlates to increased bacterial death.

Table 3

The minimum inhibitory concentration (MIC) determined from broth microdilution testing in Mueller-Hinton broth for the most effective AMP mimics

	MIC *(μg/mL)*		
Polymer	*S. aureus*	*E. coli*	*P. aeruginosa*
1. (PAPMA·Cl)	1000	1000	1000
6. (PGT25·Cl)	-	-	1000

PAPMA·Cl demonstrated the greatest antimicrobial activity, providing 100% cell death for all three of the bacteria evaluated within the therapeutic range. PAPMA·Cl's effectiveness against *P. aeruginosa* is of particular significance because of this bacteria's reported extreme resistance to traditional therapeutics.[36] In general, antimicrobial activity decreased with increasing GPMA content, and only the copolymer with the lowest GPMA concentration (PGPMA25·Cl) showed 100% cell death within the therapeutic range. Additionally, copolymers prepared with the TFA counterion showed lower activity than those associated with the chloride counterion. This is attributed to the greater coordination and bulk of the TFA counterion, which effectively shields the cation and reduces interaction with the negatively charged bacterial membrane.

Recognizing that the measured MIC value depends on the testing conditions, including media and broth type, buffer, and salt type and content,[31] copolymer effectiveness was also evaluated in low salt LB against *E. coli* and *S. aureus*. The results of these tests are found in *Table 4*. In contrast to the findings observed in MHB, all copolymers show MICs in the therapeutic range against *S. aureus* and *E. coli* when tested in low salt LB. This suggests that the decrease in salt content allowed increased

interaction of the AMPs with the bacterial membrane. All copolymers appear equally effective against *S. aureus*, but the polymers with GPMA content greater than 75 mole % show greater effectiveness against *E. coli* in the low salt environment, even when paired with the TFA counterion. The increased effectiveness of GPMA rich polymers against *E. coli* as opposed to APMA rich polymers, is attributed to mechanistic differences between the guanidinium and primary amine moiety in bacterial cell death. The membrane disrupting mechanism of APMA requires a critical concentration to sustain a hole in the bacterial membrane and, thus, achieve MIC.[32] The cell penetration mechanism of GPMA requires fewer units to translocate across bacterial membranes.[40]

Table 4

The minimum inhibitory concentration (MIC) determined from broth microdilution testing in low salt Luria broth

	MIC *(μg/mL)*	
Polymer	*S. aureus*	*E. coli*
1. (PAPMA·Cl)	300	300
2. (PGT25·TFA)	300	300
3. (PGT50·TFA)	300	300
4. (PGT75·TFA)	300	150
5. (PGT100·TFA)	300	70

Thus, these results indicate that incorporation of GPMA into APMA polymers does not generally improve the antimicrobial activity. APMA rich polymers and copolymers with chloride counterions show the most consistent antibacterial activity against the broadest range of Gram-positive and Gram-negative bacteria. In a low salt environment, however, GPMA rich copolymers demonstrate increased effectiveness

against EC, which is attributed to mechanistic differences between guanidinium and primary amine moieties.

Hemolysis Assay

Selectivity testing against red blood cells (RBCs) was performed for all polymers at concentrations 50, 500, 1000 and 3000 µg/mL (*Figure 20*). Hemolysis testing monitored the percent release of hemoglobin from RBCs as they lysed in comparison to a positive and negative control. For all polymers, at all concentrations, RBC lysis is below 10%, indicating low eukaryotic toxicity at desired antimicrobial concentrations (~1000 µg/mL). In general, hemolysis increases with polymer concentration, and the GPMA-containing polymers show greater hemolysis than the PAPMA homopolymer. Hemolysis also increases with increasing GPMA content. This may be attributed to the lower polarity of the GPMA molecule in comparison to the APMA molecule. No clear differences are observed for the copolymers prepared with TFA vs Cl counterions.

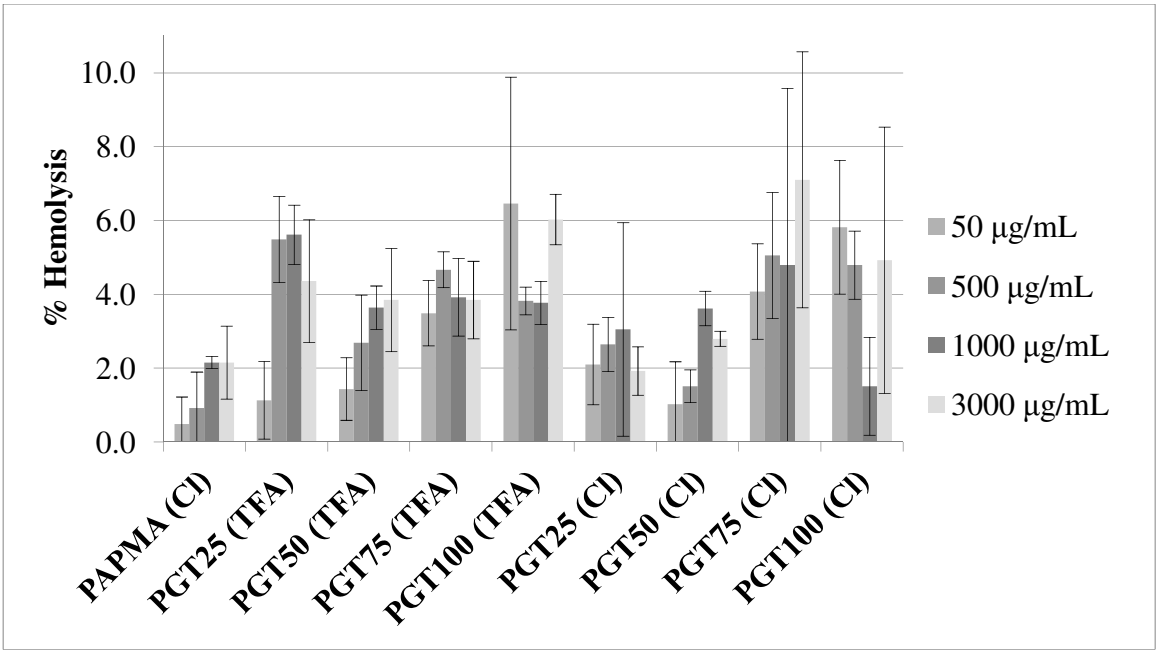

Figure 20. Hemolysis testing, where % hemolysis of red blood cells as a function of relevant antimicrobial concentrations is shown for all synthesized AMP mimics.

MTT Assay

The MTT assay utilized MCF-7 breast cancer cells as the representative eukaryotic cell for selectivity testing. *Figure 21* shows plots of % viability of MCF-7 cells as a function of polymer concentration after incubation for six hours (a) and 12 hours (b). After six hours, greater than 70% cell viability is demonstrated for solutions of PAPMA homopolymer and PGT50 copolymers with both chloride and TFA counterions at concentrations up to 2000 μg/mL. Exposure to the PGT homopolymers, however, results in dramatically reduced cell viability. Similar results are observed after 12 hours of incubation, however the PAPMA homopolymer display slightly higher cell viability than the PGT50 copolymers. No clear difference is observed for polymers produced with different counterions. As in the hemolysis testing, the increased eukaryotic cell death caused by the GPMA polymers is attributed to their less polar character, in comparison to that of the APMA molecule.

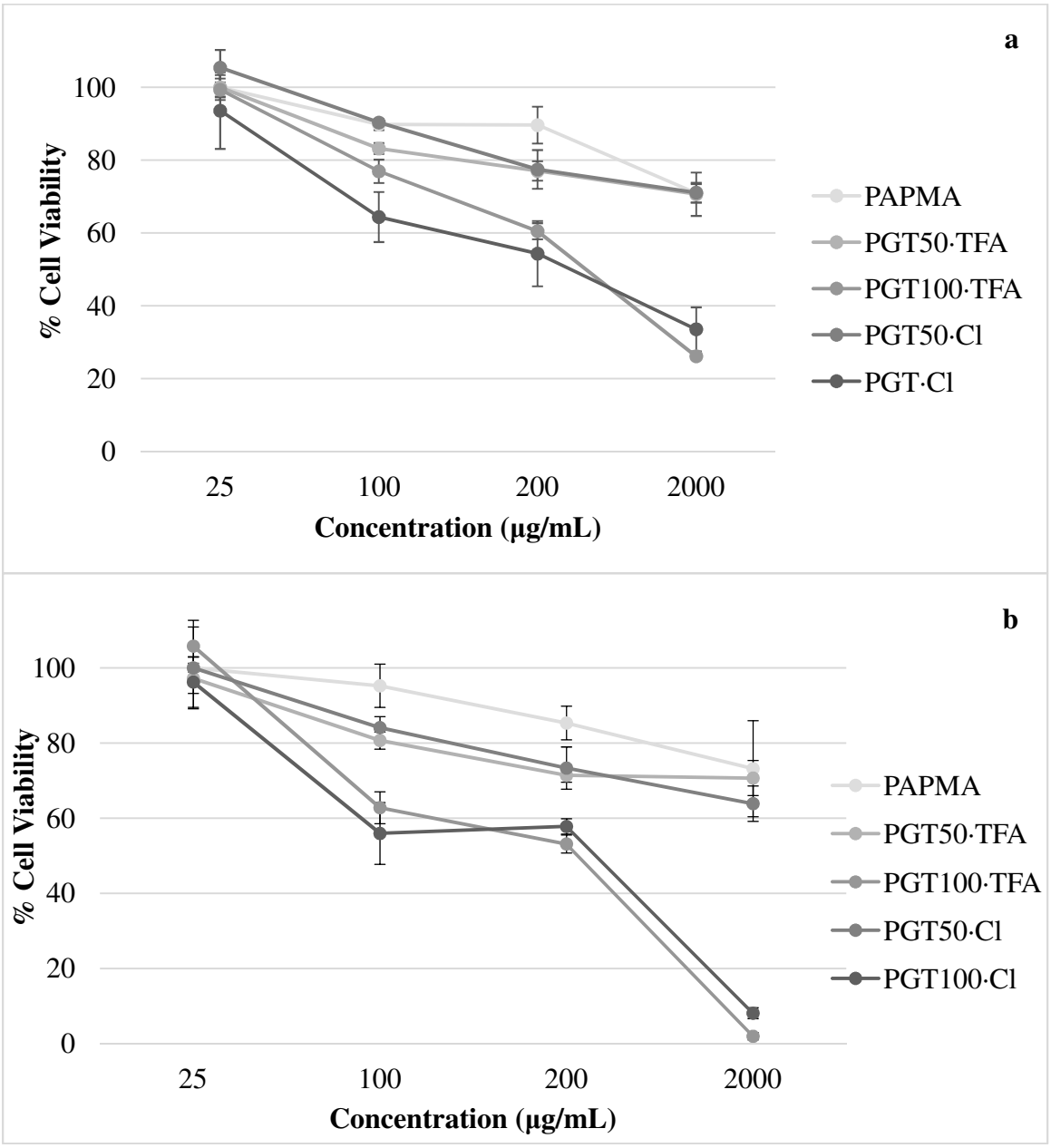

Figure 21. MTT Assay for select AMP mimics, where % cell viability of MCF-7 cancer cells as a function of relevant antimicrobial concentrations is shown after incubation for (a) 6 hrs and (b) 12 hrs.

Chapter Summary

GPMA was synthesized and polymerized with APMA via aqueous RAFT to produce homopolymers and copolymers with narrow molecular weight distribution, DP of 30, and desired copolymer composition. Antimicrobial activity was evaluated against Gram

negative *E. coli* and *P. aeruginosa* and Gram positive *S. aureus*. Selectivity was evaluated via hemolysis and MCF-7 cell viability testing. The PAPMA homopolymer demonstrated the greatest antimicrobial activity and selectivity of the copolymers evaluated, indicating its potential as a broad spectrum antibiotic. Effectiveness against *P. aeruginosa* was particularly remarkable due to its resistance to traditional therapeutics. Only copolymers with a low concentration of GPMA showed antimicrobial activity in MHB, and GPMA copolymers with Cl counterion showed greater antimicrobial activity than those with TFA counterion. When investigated in low salt LB, GPMA showed equivalent effectiveness against *S. aureus* and greater effectiveness against *E. coli* in comparison to that of APMA, demonstrating the salt sensitivity of the GPMA molecule. Eukaryotic cell death increased with increasing GPMA content. Broad spectrum antimicrobial activity and selectivity were demonstrated for fully water-soluble, primary-amine containing, methacrylamide polymers, without the need for incorporation of guanadinium adducts. Evaluation of their effectiveness in preventing bacterial biofilm formation is underway.

Recommendations for Future Work

Synthesis of APMA and GPMA polymers with lower molecular weights is recommended. This will, hopefully, decrease the concentration of polymeric AMP needed for complete cell death and allow for end groups investigation on antimicrobial activity and selectivity for PAPMA·Cl. Namely, the effect of alkyl chains of varying lengths added at the carboxylic terminal of the polymer will be analyzed to investigate the hydrophobic impact of end groups on bacterial cell death. Also, decreased molecular weight will, hopefully, allow PGT polymers to utilize the alternate bacterial cell death

mechanism supported in low salt LB and other works. If effective antimicrobial activity is achieved after decreasing the MW of PGT polymers, the tunability of APMA and GPMA copolymers can then be better evaluated. If altering the molecular weight of PGT polymers does not increase observed antimicrobial activity, incorporation of hydrophobicity through copolymerization of GPMA with monomers that have pendant aliphatic chains could be done to improve the hydrophilic/hydrophobic balance.

CHAPTER VI

CONCLUSIONS

This work has utilized acrylamide based biomimetic polymers of specific architectures to evaluate (1) the impact of specific saccharides of GM1 ganglioside on the aggregation size and kinetics of Aβ monomers and (2) the antimicrobial activity and selectivity of lysine and arginine functionalities. The key contributions from the first section are as follows:

1. Synthesis of 2-(β-D-galactosyloxy)ethyl acrylamide (GalEAm) and 2-(β-D-glucosyloxy)ethyl acrylamide (GlcEAm) as novel glycomonomers with attachment of the acrylamide backbone to the Cl' carbon of the pendant saccharide predominately in the β-orientation, increasing the biological relevance.
2. Polymerization of a series of GalEAm and GlcEAm homopolymers and copolymers with DMA, via aRAFT, to form a novel glycopolymer platform that has increased solubility and stability over a wide range of pH.
3. Determination of aggregation kinetics and aggregate size of Aβ in the presence of glycopolymer. Low MW polymers of GalEAm and GlcEAm increased the lag time of Aβ aggregation as compared to Aβ incubated without glycopolymers but eventually resulted in highly aggregated species. High MW PGalEAm decreased the lag time and hindered Aβ aggregation from proceeding past high MW oligomers. High MW PGlcEAm increased the lag time and resulted in a mixture of high MW oligomer, low MW oligomer and monomer. Low MW oligomer is thought to be more toxic. Over all, the differences seen as a result of polymer MW indicate that a concentration of saccharide greatly influences aggregation

behavior. Additionally, the stereochemistry at the C4' carbon, which is the difference between glucose and galactose, results in aggregation of species considered more toxic.

The key contributions from the second section include:

1. Improved synthesis of GPMA that allows for increased ease of production and yield.
2. Expansion of our established acrylamide based antimicrobial peptide platform to include an arginine mimic, GPMA, as well as a lysine mimic, APMA. Well defined statistical copolymers of GPMA and APMA were polymerized via aRAFT to enable investigation of antimicrobial activity and selectivity of GPMA over a range of bacteria.
3. PAPMA demonstrated the best antimicrobial activity in MHB, effectively killing *E. coli, S. aureus,* and *P. aeruginosa* which is particularly resistant to current therapeutics. Only statistical copolymers with low incorporation of GPMA and the Cl counterion were active in MHB. Use of low salt LB, showed that a high presence of GPMA in copolymers increased activity against *E. coli*. Broth type and counterion greatly impact GPMA due to the delocalization of charge across the guanidinium moiety.
4. Selectivity testing against human red blood cells and cancer cells indicate that the synthesized polymers do not harm eukaryotic cells within relevant therapeutic concentrations. Polymers rich in GPMA were slightly more toxic due to delocalization of charge across the guanidinium moiety.

REFERENCES

1. Castellani, R. J.; Rolston, R. K.; Smith, M. A., Alzheimer disease. *Dis Mon* **2010,** *56* (9), 484-546.

2. Gellermann, G. P.; Byrnes, H.; Striebinger, A.; Ullrich, K.; Mueller, R.; Hillen, H.; Barghorn, S., Aβ-globulomers are formed independently of the fibril pathway. *Neurobiol. Dis.* **2008,** *30* (2), 212-220.

3. Williams, T. L.; Day, I. J.; Serpell, L. C., The Effect of Alzheimer's Aβ Aggregation State on the Permeation of Biomimetic Lipid Vesicles. *Langmuir* **2010,** *26* (22), 17260-17268.

4. Findeis, M. A., The role of amyloid β peptide 42 in Alzheimer's disease. *Pharmacol. Ther.* **2007,** *116* (2), 266-286.

5. Kumar, A.; Bullard, R. L.; Patel, P.; Paslay, L. C.; Singh, D.; Bienkiewicz, E. A.; Morgan, S. E.; Rangachari, V., Non-esterified fatty acids generate distinct low-molecular weight Amyloid-β (Aβ42) oligomers along pathway different from fibril formation. *PLoS One* **2011,** *6* (4), e18759.

6. Yuan, C.; Johnston, L. J., Distribution of ganglioside GM1 in L-α-dipalmitoylphosphatidylcholine/cholesterol monolayers: a model for lipid rafts. *Biophys. J.* **2000,** *79* (5), 2768-2781.

7. Yanagisawa, K.; Ihara, Y., GM1 ganglioside-bound amyloid β-protein in Alzheimer's disease brain. *Neurobiol. Aging* **1998,** *19* (Suppl. 1, Proceedings of the 11th Annual Tokyo Institute of Psychiatry International Symposium, 1997), S65-S67.

8. Choo-Smith, L.-P. i.; Surewicz, W. K., The interaction between Alzheimer amyloid β(1-40) peptide and ganglioside GM1-containing membranes. *FEBS Lett.* **1997,** *402* (2,3), 95-98.

9. Matsuzaki, K., How Do Membranes Initiate Alzheimer's Disease? Formation of Toxic Amyloid Fibrils by the Amyloid β-Protein on Ganglioside Clusters. *Acc. Chem. Res.* **2014,** *47* (8), 2397-2404.

10. Yamamoto, N.; Hirabayashi, Y.; Amari, M.; Yamaguchi, H.; Romanov, G.; Van Nostrand, W. E.; Yanagisawa, K., Assembly of hereditary amyloid β-protein variants in the presence of favorable gangliosides. *FEBS Lett.* **2005,** *579* (10), 2185-2190.

11. Patel, D. A.; Henry, J. E.; Good, T. A., Attenuation of β-amyloid-induced toxicity by sialic-acid-conjugated dendrimers: Role of sialic acid attachment. *Brain Res.* **2007,** *1161*, 95-105.

12. Fung, J.; Darabie, A. A.; McLaurin, J., Contribution of simple saccharides to the stabilization of amyloid structure. *Biochem. Biophys. Res. Commun.* **2005,** *328* (4), 1067-1072.

13. Matsumoto, E.; Yamauchi, T.; Fukuda, T.; Miura, Y., Sugar microarray via click chemistry: molecular recognition with lectins and amyloid β (1-42). *Sci. Technol. Adv. Mater.* **2009,** *10* (3), No pp. given.

14. Alidedeoglu, A. H.; York, A. W.; Rosado, D. A.; McCormick, C. L.; Morgan, S. E., Bioconjugation of D-glucuronic acid sodium salt to well-defined primary amine-containing homopolymers and block copolymers. *J. Polym. Sci., Part A: Polym. Chem.* **2010,** *48* (14), 3052-3061.

15. (a) Albertin, L.; Stenzel, M.; Barner-Kowollik, C.; Foster, L. J. R.; Davis, T. P., Well-Defined Glycopolymers from RAFT Polymerization: Poly(methyl 6-O-methacryloyl-α-D-glucoside) and Its Block Copolymer with 2-Hydroxyethyl Methacrylate. *Macromolecules* **2004,** *37* (20), 7530-7537; (b) Lowe, A. B.; Sumerlin, B. S.; McCormick, C. L., The direct polymerization of 2-methacryloxyethyl glucoside via aqueous reversible addition-fragmentation chain transfer (RAFT) polymerization. *Polymer* **2003,** *44* (22), 6761-6765.

16. Ambrosi, M.; Batsanov, A. S.; Cameron, N. R.; Davis, B. G.; Howard, J. A. K.; Hunter, R., Influence of preparation procedure on polymer composition: synthesis and characterization of polymethacrylates bearing β-D-glucopyranoside and β-D-galactopyranoside residues. *J. Chem. Soc., Perkin Trans. 1* **2002,** (1), 45-52.

17. Parry, A. L.; Clemson, N. A.; Ellis, J.; Bernhard, S. S. R.; Davis, B. G.; Cameron, N. R., 'Multicopy Multivalent' Glycopolymer-Stabilized Gold Nanoparticles as Potential Synthetic Cancer Vaccines. *J. Am. Chem. Soc.* **2013,** *135* (25), 9362-9365.

18. Convertine, A. J.; Benoit, D. S. W.; Duvall, C. L.; Hoffman, A. S.; Stayton, P. S., Development of a novel endosomolytic diblock copolymer for siRNA delivery. *J. Controlled Release* **2009,** *133* (3), 221-229.

19. Vasilieva, Y. A.; Scales, C. W.; Thomas, D. B.; Ezell, R. G.; Lowe, A. B.; Ayres, N.; McCormick, C. L., Controlled/living polymerization of methacrylamide in aqueous media via the RAFT process. *J. Polym. Sci., Part A: Polym. Chem.* **2005,** *43*, 3141-3152.

20. Kumar, A.; Paslay, L. C.; Lyons, D.; Morgan, S. E.; Correia, J. J.; Rangachari, V., Specific Soluble Oligomers of Amyloid-β Peptide Undergo Replication and Form Non-fibrillar Aggregates in Interfacial Environments. *J. Biol. Chem.* **2012,** *287* (25), 21253-21264.

21. Bubb, W. A., NMR spectroscopy in the study of carbohydrates : characterizing the structural complexity. *Concepts Magn. Reson., Part A* **2003,** *19A* (1), 1-19.

22. (a) McLeary, J. B.; Calitz, F. M.; McKenzie, J. M.; Tonge, M. P.; Sanderson, R. D.; Klumperman, B., Beyond Inhibition: A 1H NMR Investigation of the Early Kinetics of RAFT-Mediated Polymerization with the Same Initiating and Leaving Groups. *Macromolecules* **2004,** *37* (7), 2383-2394; (b) Thomas, D. B.; Convertine, A. J.; Myrick, L. J.; Scales, C. W.; Smith, A. E.; Lowe, A. B.; Vasilieva, Y. A.; Ayres, N.; McCormick, C. L., Kinetics and Molecular Weight Control of the Polymerization of Acrylamide via RAFT. *Macromolecules* **2004,** *37* (24), 8941-8950.

23. Cauet, S. I.; Wooley, K. L., Kinetic investigation of the RAFT polymerization of p-acetoxystyrene. *J. Polym. Sci., Part A: Polym. Chem.* **2010,** *48* (12), 2517-2524.

24. Yeaman, M. R.; Yount, N. Y., Mechanisms of antimicrobial peptide action and resistance. *Pharmacol. Rev.* **2003,** *55* (1), 27-55.

25. (a) Yount, N. Y.; Yeaman, M. R., Emerging themes and therapeutic prospects for anti-infective peptides. *Annu. Rev. Pharmacol. Toxicol.* **2012,** *52*, 337-360; (b) Fjell, C. D.; Hiss, J. A.; Hancock, R. E. W.; Schneider, G., Designing antimicrobial peptides: form follows function. *Nat. Rev. Drug Discovery* **2012,** *11* (1), 37-51.

26. Lienkamp, K.; Madkour, A. E.; Musante, A.; Nelson, C. F.; Nusslein, K.; Tew, G. N., Antimicrobial Polymers Prepared by ROMP with Unprecedented Selectivity: A Molecular Construction Kit Approach. *J. Am. Chem. Soc.* **2008,** *130* (30), 9836-9843.

27. (a) Ikeda, T.; Yamaguchi, H.; Tazuke, S., New polymeric biocides: synthesis and antibacterial activities of polycations with pendant biguanide groups. *Antimicrob. Agents Chemother.* **1984,** *26* (2), 139-44; (b) Kuroda, K.; DeGrado, W. F., Amphiphilic Polymethacrylate Derivatives as Antimicrobial Agents. *J. Am. Chem. Soc.* **2005,** *127* (12), 4128-4129; (c) Palermo, E. F.; Sovadinova, I.; Kuroda, K., Structural Determinants of Antimicrobial Activity and Biocompatibility in Membrane-Disrupting Methacrylamide Random Copolymers. *Biomacromolecules* **2009,** *10* (11), 3098-3107.

28. (a) Palermo, E. F.; Kuroda, K., Chemical Structure of Cationic Groups in Amphiphilic Polymethacrylates Modulates the Antimicrobial and Hemolytic Activities. *Biomacromolecules* **2009,** *10* (6), 1416-1428; (b) Locock, K. E. S.; Michl, T. D.; Valentin, J. D. P.; Vasilev, K.; Hayball, J. D.; Qu, Y.; Traven, A.; Griesser, H. J.; Meagher, L.; Haeussler, M., Guanylated Polymethacrylates: A Class of Potent Antimicrobial Polymers with Low Hemolytic Activity. *Biomacromolecules* **2013,** *14* (11), 4021-4031.

29. Epand, R. F.; Mowery, B. P.; Lee, S. E.; Stahl, S. S.; Lehrer, R. I.; Gellman, S. H.; Epand, R. M., Dual mechanism of bacterial lethality for a cationic sequence-random copolymer that mimics host-defense antimicrobial peptides. *J. Mol. Biol.* **2008,** *379* (1), 38-50.

30. (a) Ilker, M. F.; Nuesslein, K.; Tew, G. N.; Coughlin, E. B., Tuning the hemolytic and antibacterial activities of amphiphilic polynorbornene derivatives. *J. Am. Chem. Soc.*

2004, *126* (48), 15870-15875; (b) Gabriel, G. J.; Madkour, A. E.; Dabkowski, J. M.; Nelson, C. F.; Nusslein, K.; Tew, G. N., Synthetic mimic of antimicrobial peptide with nonmembrane-disrupting antibacterial properties. *Biomacromolecules* **2008,** *9* (11), 2980-2983.

31. Paslay, L. C.; Abel, B. A.; Brown, T. D.; Koul, V.; Choudhary, V.; McCormick, C. L.; Morgan, S. E., Antimicrobial Poly(methacrylamide) Derivatives Prepared via Aqueous RAFT Polymerization Exhibit Biocidal Efficiency Dependent upon Cation Structure. *Biomacromolecules* **2012,** *13* (8), 2472-2482.

32. Brogden, K. A., Antimicrobial peptides: Pore formers or metabolic inhibitors in bacteria? *Nat. Rev. Microbiol.* **2005,** *3* (3), 238-250.

33. Henriques, S. T.; Melo, M. N.; Castanho, M. A. R. B., Cell-penetrating peptides and antimicrobial peptides: How different are they? *Biochem. J.* **2006,** *399* (Copyright (C) 2010 American Chemical Society (ACS). All Rights Reserved.), 1-7.

34. Treat, N. J.; Smith, D.; Teng, C.; Flores, J. D.; Abel, B. A.; York, A. W.; Huang, F.; McCormick, C. L., Guanidine-containing methacrylamide (Co)polymers via aRAFT: Toward a cell-penetrating peptide mimic. *ACS Macro Lett.* **2012,** *1* (1), 100-104.

35. Lienkamp, K.; Madkour, A. E.; Kumar, K.-N.; Nuesslein, K.; Tew, G. N., Antimicrobial Polymers Prepared by Ring-Opening Metathesis Polymerization: Manipulating Antimicrobial Properties by Organic Counterion and Charge Density Variation. *Chem. - Eur. J.* **2009,** *15* (43), 11715-11722, S11715/1-S11715/13.

36. Strateva, T.; Yordanov, D., Pseudomonas aeruginosa - a phenomenon of bacterial resistance. *J. Med. Microbiol.* **2009,** *58* (9), 1133-1148.

37. Knauf, M. J.; Bell, D. P.; Hirtzer, P.; Luo, Z. P.; Young, J. D.; Katre, N. V., Relationship of effective molecular size to systemic clearance in rats of recombinant interleukin-2 chemically modified with water-soluble polymers. *J. Biol. Chem.* **1988,** *263* (29), 15064-70.

38. CLSI, Methods for dilution antimicrobial susceptibility tests for bacteria that grow aerobically; Approved Standard-Ninth Edition. CLSI document M07-A9. Clinical and Laboratory Standards Institute: Wayne, PA, 2012.

39. Memmi, G.; Filipe, S. R.; Pinho, M. G.; Fu, Z.; Cheung, A., Staphylococcus aureus PBP4 is essential for β-lactam resistance in community-acquired methicillin-resistant strains. *Antimicrob. Agents Chemother.* **2008,** *52* (11), 3955-3966.

40. Hancock, R. E. W.; Rozek, A., *Role of membranes in the activities of antimicrobial cationic peptides*. 2002; Vol. 206, p 143-149.